

# STUDY OF BEHAVIORS OF VARIOUS CARBONS UNDER HIGH PRESSURE AND TEMPERATURE CONDITIONS BY ELECTRO-THERMAL ANALYSIS

SHIGE HARU NAKA and SHIN-ICHI HIRANO

*Synthetic Crystal Research Laboratory and Department of Crystalline Materials Science*

(Received November 19, 1981)

## Abstract

The behaviors of various carboneous materials under high pressure and temperature conditions have been studied by monitoring in situ the change in electric current against voltage applied to the sample itself (the so-called "electro-thermal analysis) under pressure. The reproducibility of the analysis can be confirmed by controlling the dimension and the charge density of the starting carbon sample in a pressure cell.

The diamond formation was found to depend strongly on the degree of graphitization and the structural factors of the carbon material used. The higher the crystallinity and the less the deformation of the starting carbon material, the lower the onset temperature for the diamond formation under otherwise the same condition. The pressure of 120kb (12GPa) is essential to convert graphite to diamond without any induction period.

Amorphous glassy carbon with the characteristic bond nature yields graphite as a metastable phase prior to the diamond formation, even when heat-treated in the diamond stable region. In this case, diamond crystals nucleate on metastably formed graphite crystal and intergrow with increasing temperature at 90 kb (9GPa).

Carbon spherulites with different graphitizability could be synthesized by the pressure pyrolysis of appropriate organic compounds, which brings about the route to synthesize diamond at a desired rate and the improvement of the texture of intergrown diamond polycrystals formed.

## CONTENTS

|                           |     |
|---------------------------|-----|
| 1. Introduction .....     | 130 |
| 2. State of Carbons ..... | 131 |

|  |     |
|--|-----|
| 2. 1. Stable Solid Phases of Carbons .....   | 131 |
| 2. 2. Diamond Synthesis .....  | 132 |
| 3. Experimental Details .....  | 134 |
| 3. 1. Starting Materials .....   | 134 |
| 3. 2. Experimental Procedures .....  | 135 |
| 4. Behaviors of Natural and Artificial Graphites under High Pressure<br>and Temperature Conditions .....   | 136 |
| 4. 1. Introduction .....   | 136 |
| 4. 2. Experimental .....   | 136 |
| 4. 3. Results and Discussion .....   | 136 |
| 4. 3. 1. Observations of diamond formation from natural graphite ....  | 136 |
| 4. 3. 2. Diamond formation from artificial graphite and induction<br>period for crystallization of diamond .....   | 138 |
| 4. 3. 3. Validity of electro-thermal analysis .....  | 140 |
| 4. 4. Conclusions .....  | 142 |
| 5. Behavior of Glassy Carbon under High Pressure and Temperature<br>Conditions .....   | 143 |
| 5. 1. Introduction .....   | 143 |
| 5. 2. Experimental .....   | 143 |
| 5. 3. Results and Discussion .....   | 144 |
| 5. 3. 1. Process of diamond formation from glassy carbon .....   | 144 |
| 5. 3. 2. Microscopic observation of diamond formation from<br>glassy carbon .....  | 146 |
| 5. 4. Conclusions .....  | 148 |
| 6. Synthesis of Carbon Spherulites and Diamond Formation by<br>Pressure Pyrolysis of Organic Compounds .....   | 148 |
| 6. 1. Introduction .....   | 148 |
| 6. 2. Experimental .....   | 149 |
| 6. 3. Results and Discussion .....   | 149 |
| 6. 3. 1. Synthesis of non-graphitizable isotropic carbon<br>spherulites by pressure pyrolysis of divinylbenzene .....  | 149 |
| 6. 3. 2. Formation of anisotropic carbon spherulites and controls<br>of morphology and character by pressure pyrolysis of<br>desired mixture of p-terphenyl and anthracene ..... | 153 |
| 6. 3. 3. Behavior of carbon spherulites under high pressure<br>and temperature conditions .....  | 155 |
| 6. 4. Conclusions .....  | 156 |
| 7. Behavior of iron carbides under high pressure and temperature<br>conditions .....   | 157 |
| 7. 1. Introduction .....   | 157 |
| 7. 2. Experimental .....   | 158 |
| 7. 3. Results and Discussion .....   | 158 |
| 7. 4. Conclusions .....  | 160 |
| 8. Summary .....   | 161 |
| Acknowledgement .....  | 161 |
| References .....   | 162 |

## 1. Introduction

Extensive researches have been carried out on the diamond formation since the first substantiated synthesis of diamond was announced in 1955 by a group at the General Electric Company Research Laboratory. The process to synthesize diamond

from graphite with metal solvent was developed rapidly and has become one of the major sources of industrial, abrasive diamond material. In recent years, with the increasing demand for the improvement of the properties of diamond tools, attentions have been paid for the studies on the behavior of the starting carbeneous material as well as the development of the new method for the diamond synthesis under high pressure and temperature conditions. This eventually has led to the requirement for preparation of the carbeneous materials with controlled degree of crystallinity and bond nature.

Only very scarce information, however, is available on the in-situ observation of the behavior of the carbeneous materials when heated under pressure and on the synthesis of carbons with desired characters, except that the rate of the diamond formation has been only suggested to depend strongly on the kind of carbeneous material used. The desire for understanding the criterion for the suitable choice of carbon material is great.

Fortunately, the starting carbon materials for diamond synthesis are electrically conductive and yield the non-conducting diamond on transforming. This characteristic change of the electrical properties enables to follow dynamically the behavior of the carbon material by monitoring the change in electric current against voltage applied directly to the carbon sample itself under high pressure (the so-called "electro-thermal analysis" under pressure).

This paper concerns the studies on the behavior of carbeneous materials under high temperature and pressure conditions and the synthesis of the carbon spherulites with desired characters, in connection with the diamond formation.

## 2. States of Carbons

### 2. 1. Stable Solid Phases of Carbons

The best characterized crystalline states of carbon are graphite and diamond, in which each atom forms three coplanar  $sp^2$  bonds and tetrahedral  $sp^3$  bonds, respectively. Graphite is the most stable allotrope at the moderate pressure and occurs naturally but is commercially made by carbonization of organic compounds (mostly coal-tar pitch and petroleum pitch) followed by graphitization at 2000~2800°C. In normal graphite, layers of condensed aromatic carbon rings are stacked so that alternate levels lie vertically beneath one another. The structure can be described in terms of a hexagonal unit cell with  $a_0=2.456\text{\AA}$  and  $c_0=6.708\text{\AA}$ . The spacing between the layers ( $1/2c_0$ ) varies with the degree of crystallinity from 3.44Å in poorly crystalline carbons to 3.354Å in highly crystalline graphite. The interlayer spacing is close to twice the van der Waals radius for carbon in aromatic rings. Forces between the layers are slight, which accounts for the valuable lubricating properties of graphite. The interaction of  $\pi p$  electrons between the layers is responsible for the electrical conduction. The electrical conductivity parallel to the layers is comparable to that of some metals, which is high by a factor of a thousand compared with that perpendicular to the layers. A second graphite structure is known, in which three types of carbon ring layer alternate, a rhombohedral structure with  $a_0=2.456\text{\AA}$  and  $c_0=\frac{3}{2}(6.708)=10.062\text{\AA}$ . The rhombohedral graphite can be

formed partly by grinding the hexagonal graphite powder in shear stress.

Diamond is denser than graphite ( $3.514\text{g/cm}^3$  compared with  $2.26\text{g/cm}^3$ ) and is thermodynamically unstable with respect to graphite at room temperature. In diamond crystal each carbon atom is tetrahedrally linked to four equidistant neighbours and accordingly the linkage extends throughout the whole crystal. The carbon-carbon bond lengths of  $1.54\text{\AA}$  are almost the same as in a simple molecule such as  $\text{C}(\text{CH}_3)_4$  or in any saturated hydrocarbon chain. The common form of diamond is cubic but a hexagonal modification of diamond and a metallic solid phase (III) have been made. The hexagonal form of diamond is metastable and related to cubic diamond in the same way as wurtzite to zinc-blende. The characteristic properties of diamond are its highest thermal conductivity ( $20\text{W/cm}\cdot\text{K}$  at  $25^\circ\text{C}$ ) and hardness  $9000\text{--}15000\text{kg/mm}^2$  at  $25^\circ\text{C}$ ) among all crystalline substances. Pure diamond is an electrical insulator with resistivity of the order of  $10^{16}\text{ ohm}\cdot\text{cm}$  at  $24^\circ\text{C}$  but doping with boron or nitrogen converts it into p- or n- type semiconductor. The entropy of graphite is higher than that of diamond, so the stability of graphite increases with increasing temperature at moderate pressure. The transformation of diamond into graphite is slow below  $800^\circ\text{C}$  but quite rapid at  $1500^\circ\text{C}$ .

Many amorphous or glassy carbon can be also produced by controlled pyrolysis of organic compounds. These carbons are composed of the turbostratic stacking of condensed aromatic carbon layers.

## 2. 2. Diamond Synthesis

The transformation of graphite into diamond had been an aim of chemists for many years. There have been many hypotheses on the synthesis of diamonds, since Tennant (1879) had found, by his combustion experiment of diamond, that diamond is a crystalline form of elementary carbon.

In 1894, Moissan<sup>1)</sup> reported his ingenious idea that diamond would come out as the precipitating carbon from quenched liquid iron droplets saturated with carbon. It was supposed that a high internal pressure could be developed in liquid core when quenched. He claimed that he could obtain tiny refractory crystals with diamond-like properties. After his announcement, many experimenters tried to reproduce this process precisely but finally decided that the process does not yield diamond, at least, reproducibly.

The first reproducible, publicly announced success of the diamond synthesis came in 1955 when a research group at General Electric Company discovered a high pressure, high temperature process for transforming graphite to diamond<sup>2)</sup>. This successful process could be done at very high pressures and temperatures by use of molten-metal solvent catalysts, which is based on the Moissan's original idea.

Because diamond is 64% more dense than graphite, the application of high pressure would favour diamond formation. High temperature would also be required to disrupt carbon-carbon bonds in graphite and allow a rearrangement of carbon atoms, as indicated by the fact that graphite has a very high melting point. Figure 1 illustrates the phase and reaction diagram for carbon,<sup>3)</sup> wherein the various thermodynamic phase boundaries are sketched and the pressure-temperature regions in which the various reactions take place are marked in.

After diamond could be synthesized in the laboratory, it became possible to confirm the location of the graphite-diamond equilibrium line within the limits of accuracy of calibration of the pressures and temperatures. Bundy et al<sup>4)</sup> indicated that the Berman-Simons equilibrium line,<sup>5)</sup> which was calculated on the basis of

the thermodynamic data, could be extrapolated to the graphite-diamond-liquid triple point. Recently, Kennedy et al<sup>6)</sup> examined the location of the equilibrium line, taking into consideration of the precise measurement of pressure and the effect of pressure on the emf of thermocouples. Their newly determined slope of the graphite-diamond equilibrium line of 0.025kb/K is almost consistent with that of 0.027 kb/K by Berman-Simon.

As is understood on Figure 1, it is proposed that diamond crystals might form satisfactorily by cooling the liquid of carbon down to the diamond stable region at pressures above the triple point. This process could yield only a few amount of very fine grained diamond embedded in flaky graphite crystals. DeCarli

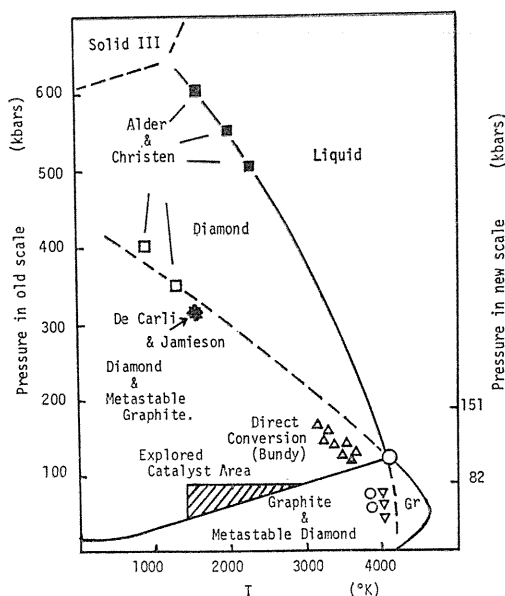


Fig. 1. Phase diagram of carbon<sup>3)</sup>.

and Jamieson<sup>7)</sup> first reported the proved instance of the direct transformation of polycrystalline graphite into diamond by shock wave compression (marked by  $\otimes$ ) with yield of a few percent of very fine diamond within microseconds. The transformation zone is located near the melting line of metastable graphite (pseudomelting). If pseudomelting takes place, the intermediate would behave like fluid and the carbon atoms could be rearranged in the stable cubic diamond form during the very short duration. A little later Bundy<sup>8)</sup> succeeded in synthesizing diamond by statically compressing graphite specimens to pressure of about 130kb (13GPa) and flash-heating them to temperatures above 3300K with a belt-type high pressure apparatus (marked by  $\triangle$  in Figure 1). The diamond formed by these processes is of the cubic type, randomly oriented crystallites, of which crystallite size was less than 100Å and 200–500Å, in the shock wave compression case and by the flash-heating at a high static pressure, respectively. Hexagonal diamond was produced by flash-heating a single crystal of graphite compressed in c-axis direction at pressures exceeding 130kb at a relatively low temperature below 2000K.<sup>9)</sup>

The direct conversion of graphite into diamond does not result in an appreciable rate of diamond formation except at very high pressures and temperatures (e. g. above 100kb, 3000K) or for longer exposing to pressures and temperatures. This behavior is consistent with the concept that the tightly bound carbon atoms of graphite crystal must be subjected to thermal agitation vigorous to disrupt the lattice and allow it to rearrange in the thermodynamically stable diamond form.

There have been some technological problems remained unsolved on the development of a high pressure and temperature apparatus which enables us to generate the pressure above 100kb in large volume for the practical use. At some intermediate pressures and temperatures, Bundy et al<sup>10)</sup> found catalysts that greatly accelerated the formation of diamond as a thermodynamically stable, and this makes

possible the commercial production of industrial diamond without prohibitively high cost for manufacturing a pressure apparatus. "The catalysts" that have been found to be effective are essentially the group VIII metals of the periodic table, such as iron, nickel, cobalt, platinum and palladium, as well as manganese, chromium and to a lesser degree, tantalum, and also alloys of the these metals.<sup>11)</sup>

A convenient procedure to synthesize diamond from graphite is to set the mixture of graphite and say nickel in a pressure cell and heat it above the nickel-

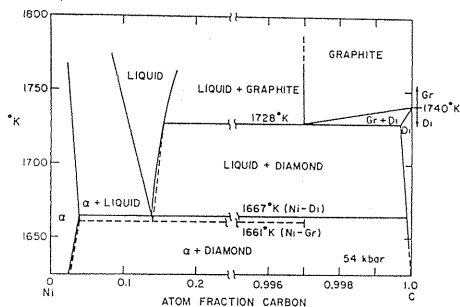


Fig. 2. Phase diagram of nickel and carbon at 54kb<sup>11)</sup>.

graphite eutectic temperature at some satisfactory pressure, such as 54 to 60kb. The nickel becomes saturated with carbon relative to graphite of the metastable phase and supersaturated relative to diamond as shown in Figure 2. Thus diamond begins to crystallize as a stable solid phase at the expense of graphite. Gem-quality diamond crystal up to 6mm could be grown on diamond seed by the careful application of this method.<sup>12)</sup> "The catalysts for the diamond synthesis" are good carbon solvents, but there are other carbon solvents which so far have not demonstrated any activity to form diamond, so that the term

"catalyst-solvent" has been customarily used for the "catalyst" to serve for the identification of the active substances.

In those catalyst-solvents mentioned above, iron might act in more complicated way and its function to form diamond has been remained unclarified. The greater the free-energy difference between starting carbon source and diamond, the greater the rate of diamond nucleation and growth. This convert led us to study about the effects of characters of carbeneous starting materials on the formation of diamond.

The other great scientific importance in this field is the diamond growth under metastable conditions. The methods that have been reported to be successful make use of diamond seedbeds as substrate and the low flux of carbon is delivered over diamond seeds at about 1300K and pressures less than atmospheric by cracking of methane gas or by molecular or iron beans of carbon.<sup>13~18)</sup> The diamond growth is thought to be epitaxial for the thin film formation and to be through VLS process for the formation of whisker.

### 3. Experimental Details

#### 3. 1. Starting Materials

The starting carbeneous materials used are listed in Table 1, in which the preheat-treatment condition and the degree of graphitization<sup>19)</sup> (P; a measure of the crystallinity of carbon) are specified. These carbon specimens were selected in order to examine the effects of the crystallinity and the bond character of the starting carbeneous materials on the diamond formation. Glassy carbon was used

Table 1. List of starting carbon materials used.

|  | Crystallite size $L_{c002}$ (Å) | Interlayer spacing $d_{002}$ (Å) | Degree of graphitization (P) |
|--|---------------------------------|----------------------------------|------------------------------|
| Natural graphite   | 1000                            | 3.354                            | 1.00                         |
| Artificial graphite (Spectroscopic grade)  | 690                             | 3.362                            | 0.90                         |
| Carbon spherulites (Synthesized by pressure pyrolysis of anthracene-paraterphenyl mixture) | 250                             | 3.400                            | 0.05                         |
| Glassy carbon (GC-20)  | 25                              | 3.460                            | 0                            |

especially with the object of the study of its behavior under high pressure and temperature conditions, because the glassy carbon has the  $sp^3$  bond nature in its structure like in diamond.

### 3. 2. Experimental Procedures

The starting carbon sample was placed in a sample cell arrangement as shown in Figure 3, and then subjected to a desired pressure up to 140kb (14GPa) in a girdle-type high pressure apparatus. The sample was heat-treated by passing the 60 cycle a. c. directly through the sample itself, and quenched to room temperature under the pressure. The applied voltage and current were measured during the heat treatment of the sample. The behavior of the carbon sample was observed dynamically by monitoring the change in the applied voltage-current relation under pressure (so-called electro-thermal analysis).

The pressure on the sample was calibrated at room temperature by detecting the changes in the electrical resistances associated with the polymorphic transitions of reference metals<sup>20,21</sup>; Bi (25.5, 77kb), Ti(36.7kb) and Ba (55, 120kb). The temperature of the sample was determined with a chromel-alumel thermocouple inserted in the central part of the sample up to 1000°C under pressure. The melting point of Ag, Au, Ni or Pt surrounded with hexagonal BN powder in the central part of carbon sample was also used as the fixed point for the determination of the relationship between the temperature and the applied electric power under pressure. The effect of the pressure on the melting points of these metals were consulted with the data by Strong et al<sup>22</sup>) and Cohen et al.<sup>23</sup>) The pressures and temperatures reported here may be in absolute error as much as 10% and in relative error by about 5%.

The specimens heat-treated under pressure were identified by the X-ray

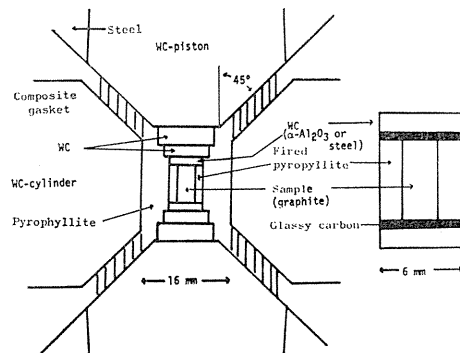


Fig. 3. High pressure cell arrangement used in this study.

diffraction method and observed under a scanning electron microscope, a transmission electron microscope and an optical microscope. The polished surfaces of sintered products were analysed with an electron probe microanalyser.

#### 4. Behaviors of natural and artificial graphites under high pressure and temperature condition

##### 4. 1. Introduction

Bundy,<sup>8)</sup> first, reported the direct conversion of graphite to diamond under static pressure, using an electric flash-heating technique. At pressures above about 125kb (old pressure scale, about 110kb on new pressure scale), he found that graphite spontaneously collapsed to nonconducting polycrystalline diamond of the cubic type with the crystallite size of 200–500Å in times of a few milliseconds or less. Naka et al<sup>24)</sup> revealed that the conversion of graphite to diamond can be detected by the drastic change in the electrical resistance of a graphite bar specimen during passing 60 cycle a. c. electric current directly through the specimen itself at 140kb. In this experiment, the diamond crystal grew up to 20µm in size.

Wentorf<sup>25)</sup> found that the amount and character of diamond converted depended strongly on the kind of the starting carbonaceous materials used. He heated various kinds of carbons to temperatures of about 1300 to 3000°C at pressures of 95 to 150 kb (or new pressure scale, 80 to 125kb) and suggested that apparently structural factors were involved and the actual transformations to diamond may have followed a number of complex reaction path. It is worthwhile from the scientific point of view to perform the in situ observation of the behavior of the starting carbon specimen during the heat treatment under pressure, which lead to finding the criterion on the selection of the carbon specimen suitable for the industrial diamond production.

In this chapter, the process of the transformations of natural and artificial graphites into diamond without any intentional addition of solvent metal has been investigated by the electro-thermal analysis. The factors influencing the sensitivity of the analysis have been discussed.

##### 4. 2. Experimental

The starting carbon specimens used were natural graphite purified with halogen gas at 2800°C and spectroscopic artificial graphite. The experimental details are mentioned in the previous chapter.

##### 4. 3. Results and Discussion

###### 4. 3. 1. Observations of diamond formation from natural graphite<sup>24)</sup>

Figure 4 shows a plot of current-voltage applied on the natural graphite specimen against time. The voltage was increased stepwise at fixed intervals. When the voltage was raised to about 1.6V at step II, a sudden increase in voltage and a decrease in the electric current were observed. This phenomenon directly reflects the formation of the non-conducting diamond from the original natural graphite.

At 120kb, when the voltage of 0.8 to 1.2V was applied, the instantaneous

decrease in the electric current could be detected as shown by an arrow ( $\leftarrow$ ) in Figure 4b, which indicates transient formation of an intermediate phase with higher electrical resistance. Beyond this transient state, the current was then increased with the increase of the applied voltage. This feature of graphite takes place only when heat-treated at pressures above 100kb, and is of great importance in relation to the formation of the metastable hexagonal diamond as reported by Bundy and Kasper.<sup>26)</sup>

The well developed flaky natural graphite crystal deformed into fragments

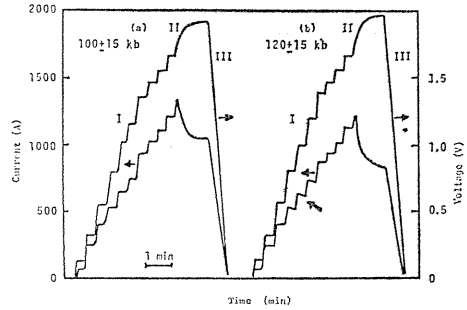


Fig. 4. Observed relation of current-voltage against time on natural graphite specimen at 100kb (a) and 120kb (b).

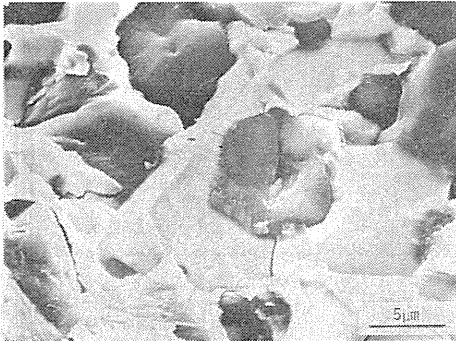


Fig. 5. Nucleation of diamond in natural graphite matrix (100kb, 2000K, 5 sec).

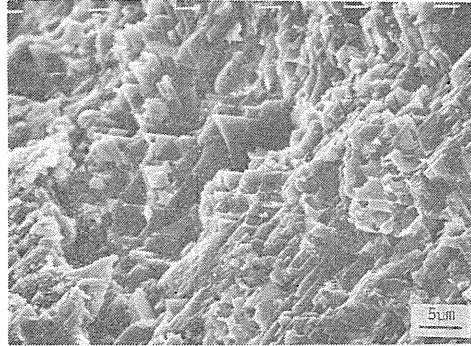


Fig. 6. Growth feature of diamond crystals (100kb, 2000K, 20 sec).

like shavings by heat-treatments at 100kb, and then the nucleation of diamond was observed in the resultant graphite matrix (Figure 5). By prolonging the heat treatment time, diamond crystals grew up along  $\langle 001 \rangle$  direction with the development of  $\{111\}$  faces (Figure 6). The remarkable change in the graphite crystal associated with the diamond formation is the abnormal decrease in the intensity of 004 X-ray diffraction in comparison with that of 002 X-ray diffraction, which appears to reflect the induced distortion or wrinkling in the treated graphite.

Grinding the natural graphite powder gives to rise the deformation in the crystal lattice, which makes the crystallinity of graphite lower. Figures 7(a) and 7(b) show the typical recorded relations of the sample current-applied voltage against time at 120kb and 1800K on a well-crystalline flaky natural graphite and on its ground specimen, respectively. The diamond formation took place at 1800K at the step II shown in Figure 7(a) on the non-ground natural graphite. The deformed natural graphite by grinding, however, could not be transformed into diamond under the same condition (Figure 7(b)). This is also recognized by the analysis of X-ray diffraction profiles as shown in Figure 8. D111 in the figure means the 111 X-ray

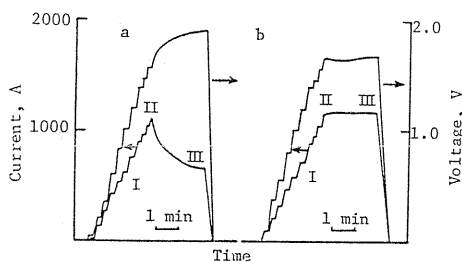
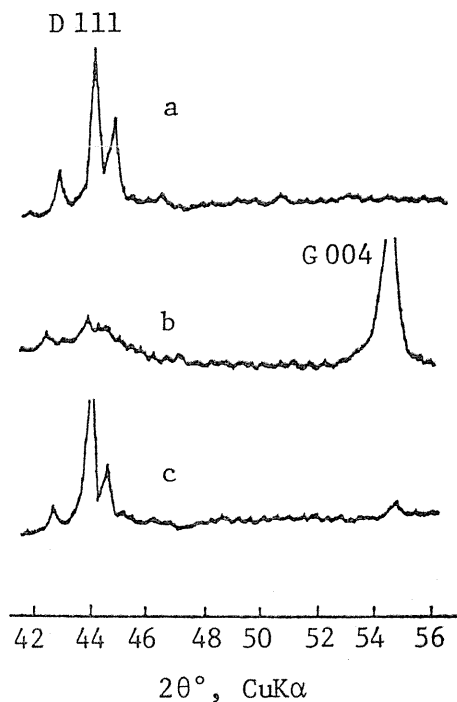


Fig. 7. Observed relation of current-voltage against time at 120kb on (a) non-ground natural graphite, and (b) ground natural graphite.

Fig. 8. X-ray diffraction profiles on  
 (a) non-ground well-crystalline natural graphite treated at 120kb and 1800K,  
 (b) ground natural graphite treated at 120kb and 1800K,  
 (c) ground natural graphite treated at 120kb and 2600K.



diffraction line of diamond. The ground natural graphite could only accept, even in the diamond stable region, the annealing effect to recover the three dimensional ordering as identified by the appearance of both the 100 and 101 diffraction lines at around  $42^\circ$  and  $44^\circ$  in  $2\theta$ , respectively (Figure 8(b)). The higher temperature of 2600K was required to transform the deformed natural graphite into diamond as shown in Figure 8(c). The result gives a suggestion that the condition for the diamond formation can be lowered to some extent by selecting the crystallinity of the starting carbon materials.

#### 4. 3. 2. Diamond formation from artificial graphite and induction period for crystallization of diamond<sup>27)</sup>

Figure 9 shows an observed typical relation of applied voltage-current against

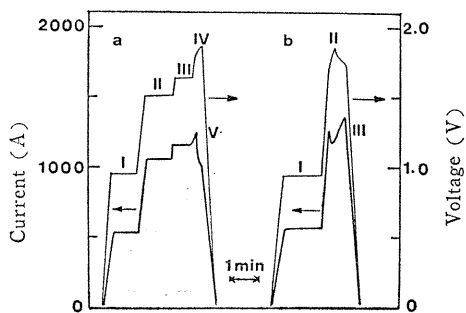


Fig. 9. Observed relation of current-voltage against time at 140kb on spectroscopic graphite bar of  $3\text{mm}\phi \times 7\text{mm}$ , (a) formation of diamond at step III to IV (b) retransformation of formed diamond to graphite at step II due to superheating.

time on the spectroscopic graphite bar of 3mm in diameter and 7mm in length at 140kb. As seen on natural graphite, the indication of the diamond formation could be detected from the recorded voltage-current relation (Figure 9(a)). Figure 9(b) illustrates the phenomena of both the diamond formation and the regraphitization of the formed diamond. At the step II, the abrupt decrease of the electrical current took place on transforming into diamond, followed by the steep increase in the current. This result seems to be attributed to the partial reconversion of the formed diamond to graphite due to the super-heating at the high resistance region where diamond was formed. It was effective to enlarge the sample diameter in order to improve the reproducibility of the diamond formation and avoid the reconversion to graphite.

Figure 10 shows the typical as-recorded relation of voltage-current against

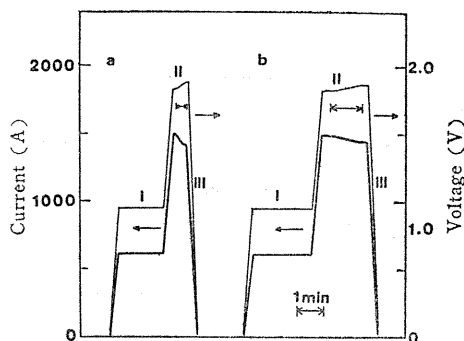


Fig. 10. Observed relation of current-voltage against time on spectroscopic graphite bar of 4mm $\phi$  $\times$ 7mm. The arrows represent the apparent crystallization time,

(a) at 115kb (b) 100kb.

time at 115kb and 100kb on a large spectroscopic graphite bar of 4mm in diameter and 7mm in length. The increase of the voltage and the decrease of the current on transforming into diamond were not so drastic as compared to the graphite bar specimen of 3mm in diameter, but the relation of current-voltage became much reproducible. As observed in Figures 10(a) and 10(b), the conversion to diamond continued for the certain time with the induction period just after setting the final applied voltage to 1.84~1.88V (corresponding to 2100~2300K) at the step II. The time for which the conversion to diamond was in equilibrium under a given condition can be called as the apparent crystallization time of diamond. The lower the applied pressure on the graphite specimen, the longer the induction period for the diamond formation. Such an apparent crystallization time is shown by an arrow in Figure 10.

The observed apparent crystallization time at around 2200K is summarized against the applied pressure in Figure 11. The conversion to diamond without any induction period is found to take place if treated above 120kb. The pressure was consistent with that reported by Bundy<sup>8)</sup> for the instantaneous conversion to diamond of graphite with the flash heating technique. The yield of diamond at around 2200K was higher than 80% at pressures above 100kb and about 50% at 90kb.

Figure 12 shows the X-ray diffraction profiles of graphite treated at 2300K and 80kb. By the heat treatment for 5min, the intensity of 004 X-ray diffraction line of graphite decreased drastically, as compared with that in Figure 12(a). The formation of diamond was observed by the heat treatment for 10min and became

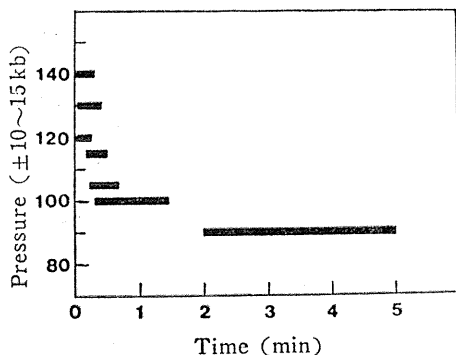


Fig. 11. Relation between apparent crystallization time of diamond and applied pressure at 2200K.

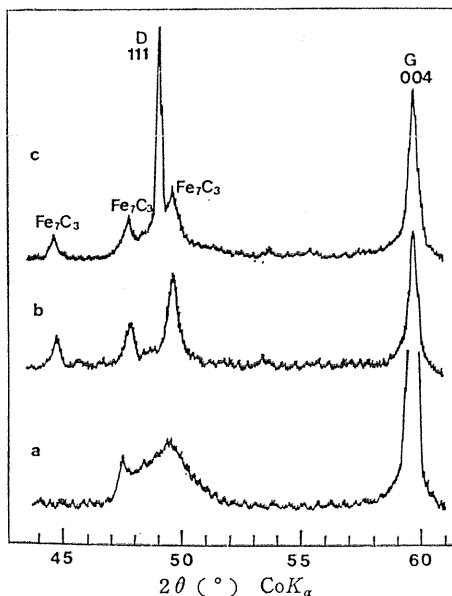


Fig. 12. X-ray diffraction profiles of spectroscopic graphite bar of 4mm $\phi$ ×7mm treated under 80kb, (a) at room temperature for 10min, (b) at 2300K for 5min, (c) at 2300K for 30min.

remarkable by prolonging the treatment to 30min. Diamond formed was associated with a foreign phase, which is identified later as  $\text{Fe}_7\text{C}_3$  solid solution with V, Cr, Mo and W. The metal constituents of SKH-9 disks in the pressure cell are conjectured to diffuse in and react with graphite sample to form the  $\text{Fe}_7\text{C}_3$  solid solution. Since the diamond formation took place instantaneously at 120kb without any induction period and crystallization time as shown in Figure 9, the influence of the coexistence of  $\text{Fe}_7\text{C}_3$  could be excluded. The role of  $\text{Fe}_7\text{C}_3$  in the diamond formation process should be clarified in detail.

#### 4. 3. 3. Validity of electro-thermal analysis

The reproducibility of the voltage-current relation and the onset condition of the diamond formation were found to depend strongly on the dimension and the charge density of the starting graphite sample with the same graphitizability. Figure 13 illustrates changes in the recorded current-voltage relations against time at 80kb with the charge density of graphite sample. Figures 13(a) and 13(b) are on weighed spectroscopic graphite bars of 220mg and 246mg, respectively, and Figures 13(c) and 13(d) on weighed graphite bars for electrode of 240mg and 247mg, respectively. The lower the charge density of the starting graphite sample, the higher electric power is required to form diamond, as seen by the comparison of Figures 11(a) with 13(b).

The same relations of current to applied voltage, in other words, the same

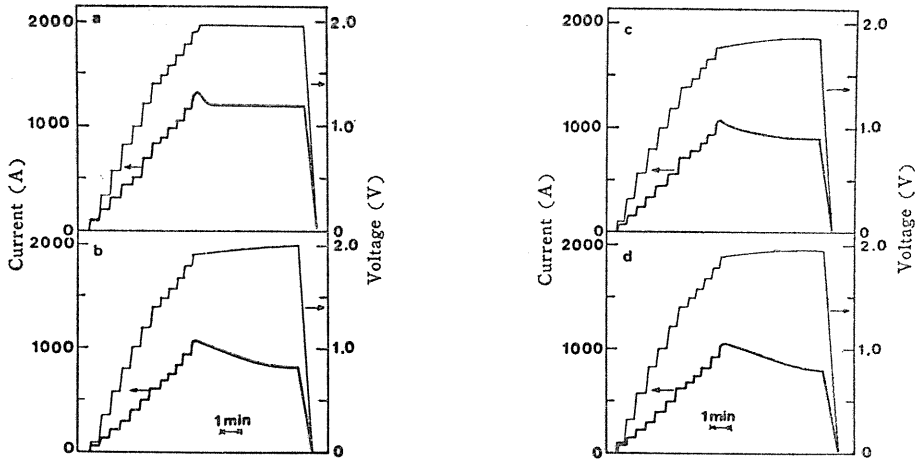


Fig. 13. Observed relation of current-voltage against time at 80kb on graphite samples with dimension of 4.5mm $\phi$  $\times$ 9mm

- (a) 220mg } spectroscopic graphite bar
- (b) 246mg }
- (c) 240mg } graphite bar for electrode
- (d) 247mg }

behaviors of the change in the electrical resistance of the specimen were observed on the samples with the same sample density as shown in Figures 13(c) and 13(d). Figures 13(b) and 13(d) also demonstrate that the same current voltage relation can be obtained reproducibly by the strict control of the charge density of graphite sample if the starting graphite samples have the same degree of graphitization as in the spectroscopic graphite and the graphite bar for electrode used in this experiment.

Figure 14 illustrates the relationships of the applied voltage and current, which

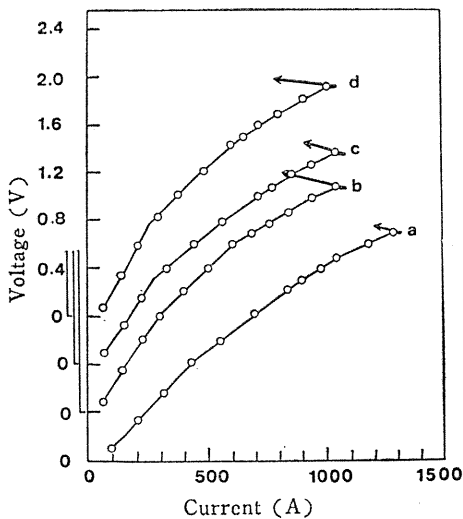


Fig. 14. Relation of applied voltage and current of sample with dimension of 4.5mm $\times$ 9mm at 80kb,

- (a) 220mg } spectroscopic graphite bar
- (b) 246mg }
- (c) 240mg } graphite bar for electrode
- (d) 247mg }

The arrows represent onset of diamond formation at which sudden decrease of electric current is observed.

are drawn by re-plotting the voltage and the current at each step in Figure 13. The arrows in Figure 12 point out the onsets of the diamond formation at which the sudden decrease in the electric current is observed.

The change in the rate of the increase of the electric current with the applied voltage, that is the change in the overall electrical resistance of the sample, becomes remarkable beyond the applied voltage of 0.8V in all graphite samples used. This change of the electrical resistance is concerned with the fact that the distortion of the original graphite introduced by pressurizing at room temperature is annealed out by the heat treatment. This annealing effect is intensified with the increase in the applied electric power till the diamond formation takes place. The behavior of the starting graphite sample can be followed dynamically by this electro-thermal analysis.

#### 4. 4. Conclusions

The transformation process of graphite to diamond without any intensive addition of metal solvent was observed dynamically by following the change in the applied voltage-current relation (so-called the electro-thermal analysis). The factors influencing the sensitivity of this analysis and the effect of crystallinity of the starting graphite on the diamond formation have been investigated in this chapter.

(1) The graphite sample must be machined into the optimum size in order to avoid the reconversion of the formed diamond to graphite by the local superheating.

(2) Under pressures below 120kb, the induction period prior to the diamond formation and the apparent crystallization time for diamond increased with the decrease of the applied pressure. The pressure of 120kb was essential to convert graphite to diamond without any induction period.

(3) The phenomena accompanied by the diamond formation could be observed reproducibly by controlling the dimension and the charge density of the starting graphite sample with the same degree of the graphitization.

(4) The diamond formation was found to depend strongly on the degree of the graphitization. The decrease in the electrical resistance of the graphite sample on heating under pressure is observed to take place owing to the annihilation of the strain introduced by the compression at room temperature. Diamond can be formed at the lower temperature from natural graphite compared with the formation temperature of diamond from artificial graphites with lower degree of graphitization.

(5) Higher temperature is required for the diamond formation when natural graphite deformed by grinding is employed instead of non-ground well crystalline natural graphite. The deformed graphite is subjected to annealing prior to the diamond formation.

(6) The electro-thermal analysis is confirmed to serve for the in situ observation of the processes of the anneal and the recrystallization of the pressurized original graphite on heating.

## 5. Behavior of glassy carbon under high pressure and temperature conditions

### 5. 1. Introduction

In the previous chapter, the diamond formation was found to depend strongly on the degree of graphitization of the starting carbon sample. In recent years the availability of a group of highly disordered carbon has gained the attention of materials engineers because of their very low density coupled with isotropic high strength and hardness at both low and extreme temperatures, and excellent corrosion resistance. These materials have been called glassy or vitreous carbon, due mostly to their physical resemblance to black glass. All of these carbons are apparently produced by the controlled thermal decomposition of crosslinked polymers. Therefore, their structure might be expected to be subject to the kind of polymer used as starting organic material, which leads to the inhomogeneities where graphite-like parts with  $sp^2$  bond nature are connected by the carbon-carbon bonding forming the diamond like  $sp^3$  hybrid orbital.

It is worthwhile to follow the evolution of structure from glassy carbon and give the conclusion to the question on whether or not the diamond like-bonds in glassy carbon may serve as the nucleation site and lower the pressure-temperature condition for the diamond formation. Previously, the authors<sup>28)</sup> found that the diamond did form on a graphite grain, which had been grown as a metastable phase at high pressures and temperatures.

In this chapter, the behavior of glassy carbon with the characteristic bond nature has been studied in its metastable region by the electro-thermal analysis and the microscopic observations.

### 5. 2. Experimental

The glassy carbon used was GC-20 powder (Tokai Carbon Co., Ltd) of the grain size in the range of 200-325 mesh. The total metallic impurities amounted to few hundreds ppm. The powder sample of 90mg was placed in the sample cell as shown in Figure 3. The experimental procedure was the same as mentioned in the previous chapter.

Two kinds of 002 X-ray diffraction profiles of carbon were observed on the specimens heat-treated under pressure. One is symmetrical as in well-crystalline graphite after the correction to the diffraction intensities for the Lorentz-polarization, atomic scattering and absorption factors. The other is a so called composite profile which indicates the coexistence of the turbostratic structure as in the original glassy carbon and the graphitic structure newly developed. The composite profiles were graphically separated into two symmetrical component profiles corresponding to each structure by the conventional method reported by Hirano<sup>29)</sup> and Noda et al.<sup>30)</sup> The amount of graphite formed from the glassy carbon was measured as the area ratio of the profile for the graphitic component to the whole composite profile, using the calibration curve drawn by the same analysis of the X-ray diffraction profiles on mixtures of given amounts of graphite and turbostratic carbon.

### 5. 3. Results and Discussion

#### 5. 3. 1. Process of diamond formation from glassy carbon<sup>31)</sup>

It was found that the glassy carbon of the turbostratic structure bonded with the criss-cross linkage could not transform directly to diamond by the heat-treatment under static pressures up to 100kb (10GPa) in the diamond stable region, but convert to diamond through the well-crystallized graphite of the metastable phase. The graphite crystals with the same interlayer spacing of 3.354Å as natural graphite could form from the glassy carbon even at temperature as low as 600°C at 40kb. The diamond formation did not take place by the treatments at temperatures up to 2800°C under 40kb and 60kb, but could be observed at 2300°C under 90kb and at 1800°C under 100 kb for 5min.

Figure 15 illustrates the voltage-current relations of the glassy carbon specimens under pressures of 65kb and 90kb. In the figure the voltage-current relation of

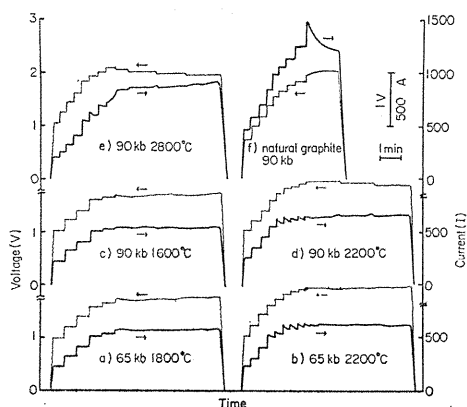


Fig. 15. Observed relation of current-voltage against time of glassy carbon GC-20 and natural graphite.

As shown in Figures 15(b), (d) and (e), the spontaneous decrease in the electric current of about 20 to 60A was observed by the application of around 1.8V (corresponding to around 1500°C), where the electric current displays the serrated change in response to applying the voltage on glassy carbon sample step-wise. Such an electric current change continued to the application of 1.95V, at which temperature of the sample was about 2000°C. This characteristic phenomenon appears to reflect the formation of the metastable hexagonal diamond as suggested in the case of natural graphite treated at 120kb. By the treatment at 2800°C under 90kb as shown in Figure 15(e), the diamond formation took place, but the decrease of the electric current was not so remarkable as compared with

that on natural graphite shown in Figure 15(f). The graphitization of the glassy carbon with the heat treatment canceled the sudden increase of the electrical resistance of the specimen associated with the diamond formation. Consequently the overall electrical resistance of the specimen was kept almost constant in spite of the diamond formation.

Figure 16 shows the observed 002 X-ray diffraction profiles on specimens treated at various temperatures under 90 kb for 5min. The X-ray diffraction profile became to be the so-called composite as the amorphous glassy carbon had been crystallized to graphite as shown on the profile at 1000°C. The profile located at higher diffraction angle corresponds to the graphitic component formed in the glassy carbon. The interlayer spacing of the graphitic component thus formed was 3.354Å of the same value as the natural graphite. This composite profile is ascribed to the heterogeneous crystallization of graphite in the amorphous carbon matrix.

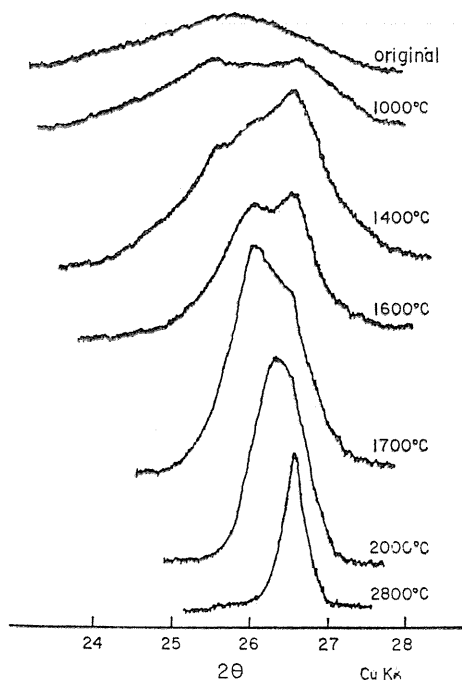


Fig. 16. X-ray diffraction profiles of specimens treated at various temperatures under 90kb for 5min.

The higher the heat treatment temperature at a given pressure, the more the amount of graphitic component formed.

Figure 17 illustrates the process of the diamond formation through the metastable graphite from the glassy carbon under 90kb. The amount of graphite (G) increased up to 2200°C with increasing the heat treatment temperature, and then gradually decreased associated with the

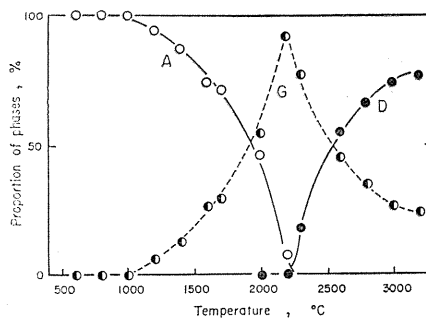


Fig. 17. Changes in amount of phases with heat treatment of glassy carbon GC-20 under 90kb  
A: amorphous glassy carbon, G: graphite, D: diamond.

diamond formation (D). It turns out that the diamond formation from the amorphous glassy carbon (A) obeys the well-known Ostwald's step rule characteristic of the contribution of the intermediate metastable phase (graphite) on transforming.

As the reference experiment, the glassy carbon and the mixture powder samples of 20w/o electro-deposited pure iron-80w/o glassy carbon were individually heat-treated at 90kb with Mo metal disk instead of steel end disk in the pressure cell, so as to examine the effect of iron diffusing from the steel end disk on the behavior of glassy carbon. As for the glassy carbon GC-20 itself, well-crystallized graphite crystals were formed at 1200°C and the amount of graphitized grains increased with the heat treatment temperature. At about 2100°C the electric current passing through the sample became unstable, probably due to the reaction of Mo metal with the glassy carbon, which made the experiments at high temperature difficult. The diamond formation could not be detected up to about 2100°C, but the metastable graphitization in the diamond stable region was confirmed to proceed as shown in Figure 16.

The glassy carbon of GC-30S preheat-treated at 2950°C did behave in the same way as GC-20, except that the higher temperature was required for the formation of the well-crystallized graphite. The diamond formation was found also not to take place prior to the metastable formation of graphite with the similar crystallinity to natural graphite.

Conclusively the diamond formation was found not to occur unless the graphite crystals with crystallinity similar to the natural graphite were formed metastably. These results indicate that the characteristic chemical bond ( $sp^3$ ) in the glassy carbon did not serve for the nucleation of diamond under the static pressure, but was broken down to rearrange as the graphitic structure with  $sp^2$  bond nature.

### 5. 3. 2. Microscopic observation of diamond formation from glassy carbon

Figure 18 manifests the feature of the process of the diamond formation from the amorphous glassy carbon under 90kb. Prior to the diamond formation, the original glassy carbon grain (Figure 18(a)) with the irregular shape like pieces of broken glasses transformed to the well crystallized graphite crystal of preferred orientation of graphitic layers as shown in Figure 18(b) by the heat treatment at 2200°C. Figure 18(c) represents the transient state at which diamond crystals nucleated on crystallized graphite grains to grow gregariously in the octahedral form along the direction restricted by the geometrical selection. The lower portion of the grain in this figure is a graphite crystal remaining untransformed. At higher temperature such as 2800°C, the developed (111) surface of diamond tends to be covered with thin growth layers composed of several growth hillocks as shown in Figure 18(d). Our experiments indicate that diamonds prefer to grow by the

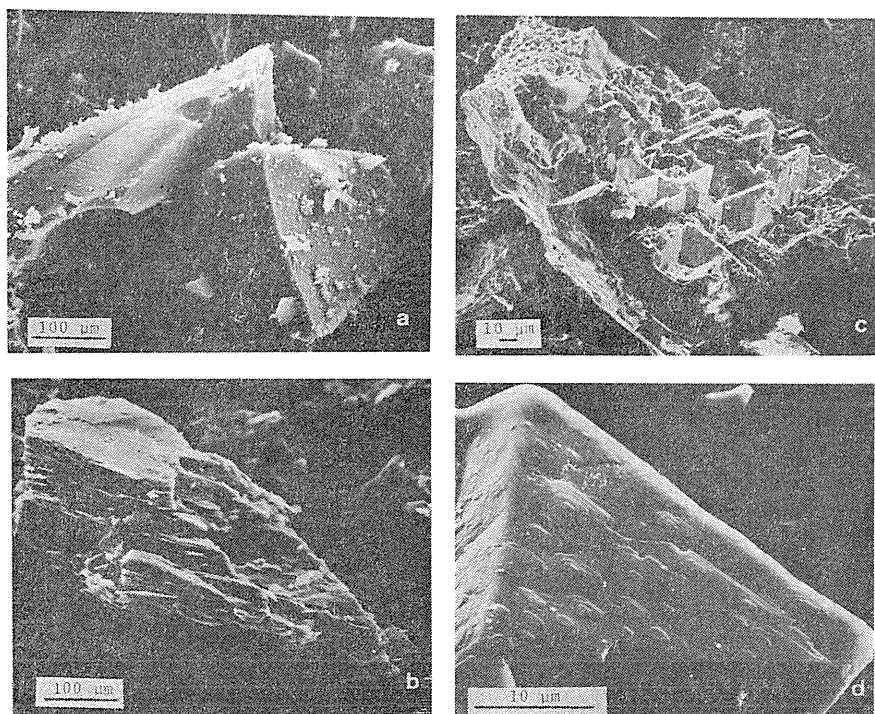


Fig. 18. Feature of diamond formation process from glassy carbon under 90kb,  
 (a) original powder  
 (b) crystallized graphite crystal with preferred orientation of graphitic layer at 2200°C  
 (c) diamond crystals formed on crystallized graphite grain at 2800°C  
 (d) surface microtopograph of diamond (111) formed at 2800°C.

pling up of layers parallel to the (111) crystallographic plane. This phenomenon has long been promoted by scientists who have examined natural diamond since there are obvious steps on the (111) faces of many natural diamonds.

On the (111) diamond face, many trigons in the same orientation can be always found to originate in some intimate way due to the growth failure on the (111) plane. Figure 19 shows the evidence of the survival of the trigons when the diamond was actually growing at the time under the conditions at 100kb and 2400 °C. The resemblance to such was also observed in laboratory, as shown in Figure 20, on the specimen heat treated at 3200°C and 90kb where diamond had intergrown very rapidly. The trigon corners point toward the edges of the octahedral faces.

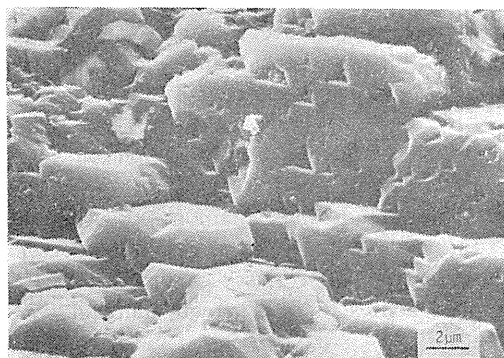


Fig. 19. Trigons on diamond (111) face formed at 2400°C under 100kb.

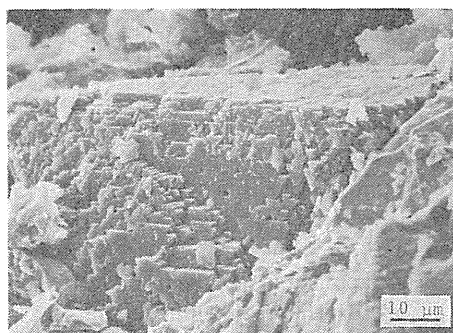


Fig. 20. Characteristic evidence of trigons on diamond formed at 3200°C under 90kb.

The origin of trigons has for long remained as a subject to be solved. Tolansky and Wilcock,<sup>32)</sup> Helperin,<sup>33)</sup> Tolansky and Sunagawa<sup>34)</sup> and Verma<sup>35)</sup> conceived trigons to have originated in growth, whereas Omar and Kenawi,<sup>36)</sup> Frank et al,<sup>37)</sup> Frank and Puttick,<sup>38)</sup> Wilks,<sup>39)</sup> Pattel and Ramanathan,<sup>40)</sup> Patel et al<sup>41)</sup> and Lang<sup>42)</sup> explained them as due to etching (dissolution) after growth. Laboratory evidence, as shown in Figures 19 and 20, indicates that trigons might be essentially a record

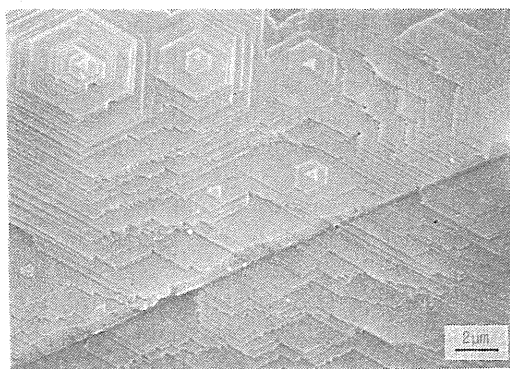


Fig. 21. Surface microtopograph of diamond (111) face grown at 2600°C under 100kb for 15min.

of the growth failure. The growth rate of diamond is very high under the conditions employed in this experiment. Therefore, it is difficult to prevent nucleation so that diamond starts growing simultaneously, which results in forming a diamond sintered body by intergrowth, similar to natural carbonado diamond.

By the heat treatment for the longer time and/or at higher temperature close to the diamond-graphite equilibrium line, diamond crystals show the tendency to be bounded with the relatively smooth (111) face, as shown in Figure 21, especially in an opening formed by the spacial reduction on transforming into diamond ( $d=3.51 \text{ g}\cdot\text{cm}^{-3}$ ) from graphite ( $d=2.26 \text{ g}\cdot\text{cm}^{-3}$ ).

#### 5. 4. Conclusions

It was found that the glassy carbon with characteristic bond nature could not be transformed directly to diamond by the heat treatment under static pressure in the diamond stable region, but to metastably formed graphite with the same degree of graphitization as natural graphite. The result revealed that diamond could form only under the contribution of the metastable graphite, according to the Ostwald's step rule.

Many growth trigons were observed on the (111) face of diamond crystals formed at high growth rates. By the treatment for longer time and/or at higher temperature close to the diamond-graphite equilibrium line, diamond crystal tend to grow with the relatively smooth (111) faces composed of thin growth layers.

The present method for the diamond formation from glassy carbon is expected to be applicable to the production of sintered bodies of intergrown diamonds with the preferred orientation of the (111) face.

## 6. Synthesis of carbon spherulites and diamond formation by pressure pyrolysis of organic compounds

### 6. 1. Introduction

In the previous chapters, it was revealed that the structural factors and the crystallinity of the starting carbon materials play an important role in the formation of diamond. The structural factors and the crystallinity of resultant carbons depends markedly on the bond character of the original organic compound, as well as on the condition of the heat treatment. Kipling et al<sup>43)</sup> reported that graphitizable carbons, which are easily crystallized to graphite crystal, are produced only when an organic compound fuses to form condensed aromatic rings during pyrolysis. Thermosetting polymer can in general yield non-graphitizable carbons. Pressure also influences solubility, viscosity, density, and phase separation and pyrolysis.<sup>44~47)</sup> Hirano et al<sup>48)</sup> first synthesized isotropic carbon spherulites by pressure pyrolysis and reported the conditions for the control of the morphology of carbons formed from divinylbenzene.<sup>48)</sup>

The adjustment of chemical bonds in carbon precursors is considered to be possible by the copolymerization or the intensive mixture of the original organic compounds with different bond character, which leads to the control of structural factors of the resultant carbons. Hirano et al<sup>49)</sup> recently found the possibility of controls of the morphology and the nature of the synthesized carbon by the copolymerization of styrene and divinylbenzene. This result has been applied to the

synthesis of the anisotropic carbon spherulites stable even at 2300°C by the pressure pyrolysis of the desired mixture of p-terphenyl and anthracene.<sup>50)</sup>

This chapter describes the experimental results on the synthesis of characteristic carbons by pressure pyrolysis of organic compounds and the behaviors of formed carbon spherulites under high pressure and temperature conditions.

## 6. 2. Experimental

The starting organic compounds used were as follows:

m- and p-divinylbenzene with 45% ethylvinylbenzene,  
styrene,  
p-terphenyl,  
anthracene.

Before pressure pyrolysis, divinylbenzene, styrene or their mixture were polymerized in a gold capsule at 300°C for 2h under 1000kg·cm<sup>-2</sup> (about 100MPa) or at 150°C for 30 min under atmospheric pressure without catalyst.

All pressure work was carried out in a hydrothermal apparatus of the cold-seal type. The starting organic materials were sealed in thin-walled gold capsules of 3.0 to 7.0mm diameter and 50mm length, and subjected to pyrolysis at selected temperatures up to 800°C under pressure up to 2000kg·cm<sup>-2</sup> (about 200MPa). Pressure was measured with a Heise gauge and temperature was controlled with a sheathed thermocouple set in the pressure vessel. The temperature was raised at 10°C min<sup>-1</sup> and quenched after an experimental run. The carbon specimens produced were further heat-treated at 2000°C or 2300°C for 1 h in flow of nitrogen. The behaviors of the heat-treated carbon specimens under high pressure and temperature conditions were also studied in the same way as mentioned in Chapter 3.

The carbons produced were characterized by X-ray diffraction and scanning electron microscopy and polarized light microscopy. The density of carbons was determined within ±0.02g·cm<sup>-3</sup> by a sink-float method. The products of pyrolysis were analysed by infra-red spectroscopy and gel-permeation chromatography (GPC).

## 6. 3. Results and Discussion

### 6. 3. 1. Synthesis of non-graphitizable isotropic carbon spherulites by pressure pyrolysis of divinylbenzene

Pressure polymerization proceeded very rapidly without the use of a catalyst and yield hard non-porous pale-yellowish pieces which were insoluble in common solvents and contained residual vinyl functional groups. The solid polymer synthesized at atmospheric pressure showed stronger infra-red absorption by vinyl groups (factor of 5).

The morphology of resultant carbon depended strongly on the pressure and temperature of pyrolysis and the nature of chemical bonds within the polymer.

From the polymer prepared by pressure polymerization a porous carbon (Fig. 22(a)) was formed under pressure below 900kg·cm<sup>-2</sup> at 615°C. Between 1000 and 1300kg·cm<sup>-2</sup>, the carbon specimen consisted of mixtures of porous carbon and coalescing carbon spherulites. The pore size in the porous carbon decreased with increasing pyrolysis pressure, from 35 to 50μm at 700kg·cm<sup>-2</sup> to 10 to 30μm at 1100kg·cm<sup>-2</sup> at 615°C. The bulk density of the porous carbon was 0.95 to 1.05g·cm<sup>-3</sup>. Isolated carbon spherulites (Figure 22(b)) could be synthesized at 1000 to 1250kg·cm<sup>-2</sup> and between 660 and 700°C, using polymers prepared at atmospheric

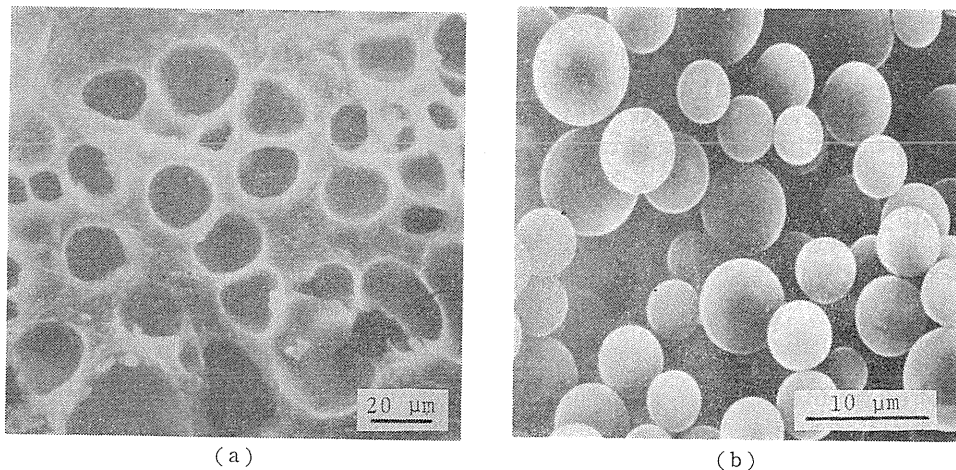


Fig. 22. Morphology of carbons formed by pressure pyrolysis of divinylbenzene.  
 (a) porous carbon fomed by pyrolysis at 615°C and 900kg·cm<sup>-2</sup> of polymer prepared at 1000kg·cm<sup>-2</sup>  
 (b) Spherulitic carbons formed by pyrolysis at 700°C and 1000kg·cm<sup>-2</sup> of polymer prepared at atmospheric pressure.

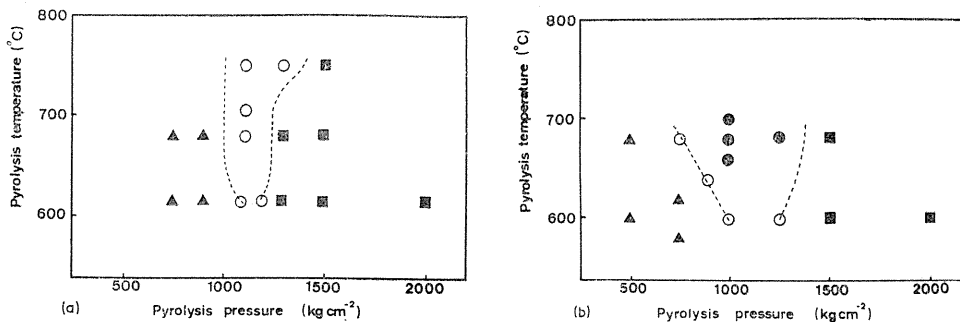


Fig. 23. Formation of carbons with various morphologies by pressure pyrolysis of polymer prepared  
 (a) at 300°C and 1000kg·cm<sup>-2</sup> for 2h  
 (b) at 150°C at atmospheric pressure for 30min  
 ▲: porous carbon, ●: spherulitic carbon, ■: coalescing spherulitic carbon, ○: mixture of porous carbon and coalescing spherulitic carbon.

pressure. The diameter of the carbon spherulite was 3 to 10 $\mu$ m with a density of 1.55 to 1.57g·cm<sup>-3</sup>. The spherulites coalesced during pressure pyrolysis above 1500kg·cm<sup>-2</sup>. Figure 23 summarized the conditions for formation of several morphologies of resultant carbon.

The carbon specimens obtained from divinylbenzene were optically isotropic.

Important effect in pressure pyrolysis is the high carbon yield of the order of 80% of the charged polymer as compared with about 10% by pyrolysis of the same polymer in nitrogen, as well as the possibility of control over the morphology of the carbons.

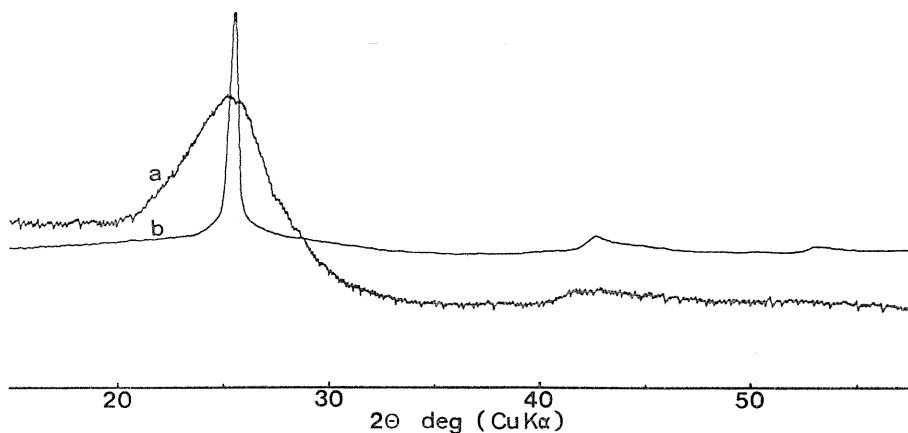


Fig. 24. X-ray diffraction profiles of spherulitic carbon before and after heat treatment at 2000°C for 1h  
 (a) original spherulitic carbons before heating  
 (b) carbons after heating at 2000°C.

These spherulitic carbons retained their morphology and isotropy after heat treatment to 2000°C, with a weight loss of about 7%. The spherical shape does not change on heat treatment unlike the anisotropic spheres which show extensive cracking.<sup>4,7)</sup> Figure 24 shows the X-ray diffractions on the carbon spherulites, of heat treatment temperatures at 700 and 2000°C. The interlayer spacing was 3.44Å and crystallite size was 120Å at 2000°C.

The isotropy and non-graphitizable properties of the carbon spherulites are attributable to the "disordered" criss-cross linkage of carbon-carbon bonding in the polymer. The following changes were observed:

- (1) the polymer began to decompose above 410°C and the vinyl functional group of the original polymer disappeared,
- (2) there was a decrease in the number of methylene groups from 410°C to about 580°C,
- (3) meta(m)- and para(p)-disubstituted benzene rings (different from the original polymer) appeared about 440°C at which a homogeneous fluid was formed with molecular weights less than 5000amu,
- (4) ortho(o)-disubstituted benzene rings formed at the later stages of thermal decomposition and then gradually increased so leading to condensed aromatic rings and subsequently to the development of a turbostratic structure,
- (5) at 530°C, the fluid matrix tended to coexist with a wax-like substance made up of components of molecular weight above 10000amu which cause the increase in the number of o-substrated benzene ring, as shown in Figure 25(b),
- (6) the survival of carbon-carbon cross-linkage in the original polymer was observed even by the treatment at 580°C, which prevents the development of large two-dimensional graphite layers. Figure 25(c) models schematically a structure for the isotropic, turbostratic non-graphitizable carbon from divinylbenzene.

These results suggest that the liquid-liquid microphase separation must be of importance for the formation of the carbon spherulites. The higher molecular weight components nucleate as liquid droplets in the fluid matrix. The droplets

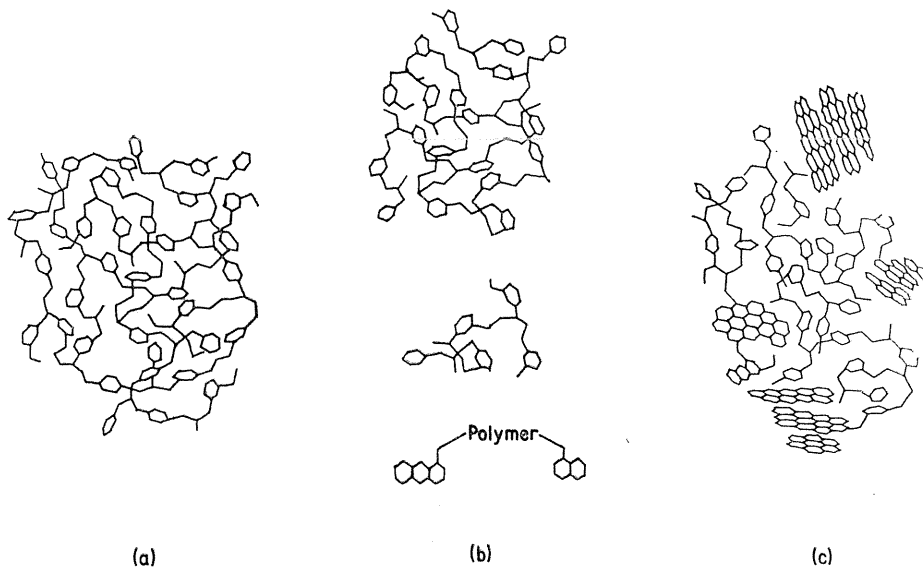


Fig. 25. Schematic drawing of structural changes in pressure pyrolysis of polyvinylbenzene  
 (a) original polymer  
 (b) intermediate state (phase separation of pyrolysis liquid)  
 (c) carbon formed

grow, remaining suspended in the fluid matrix as the pyrolysis continues. The phenomenon of irreversible spherulitic carbon formation may be similar to reversible microphase separation in spinodal decomposition in glass-forming systems.

If the formation mechanism of carbons by pressure pyrolysis mentioned above would be accepted, the morphology and nature of the formed carbon can be controlled by the control of carbon-carbon bondings in the original copolymer. Figure 26 illustrates the morphological change of the carbons formed by the pressure

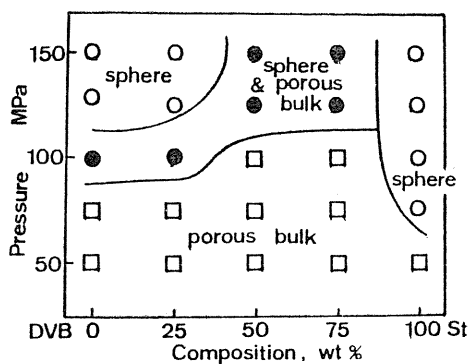


Fig. 26. Morphological change of formed carbons with pyrolysis condition and copolymerization of divinylbenzene and styrene.

pyrolysis of divinylbenzene-styrene copolymers. The kind of chemical bond in the starting polymer could also influence the character of the formed carbon. Carbons formed by the pyrolysis of copolymers rich in styrene were optically anisotropic and tended to crystallizing to graphite (being graphitizable) by heat-treatment at 2000°C, while carbons from copolymers rich in divinylbenzene were isotropic and non-graphitizable. The survival of criss-cross linkages in the polymer during pyrolysis is the origin of the difficulty of the development of the large graphitic layer.

6. 3. 2. *Formation of anisotropic carbon spherulites and controls of morphology and character by pressure pyrolysis of desired mixture of p-terphenyl and anthracene*

Carbons formed from anthracene showed the optically anisotropic and graphitizable character, and changed their morphology towards the spherule with the increase of the pyrolysis pressure. The anisotropic mesophase carbon spherulites formed intermediately during the pyrolysis readily coalesced on heating under the moderate pressure of  $300\text{kg}\cdot\text{cm}^{-2}$  (30MPa) to show the complete mosaic texture as shown in Figure 27(a). The increase of the pyrolysis pressure restrains the coalescence of the mesophase carbon spherulites to give only the isolated anisotropic carbon spherules at  $2000\text{kg}\cdot\text{cm}^{-2}$  (Figure 27(b)).

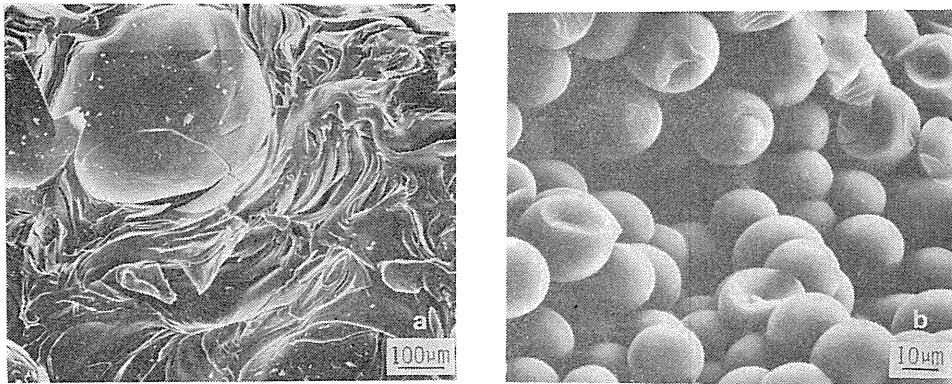
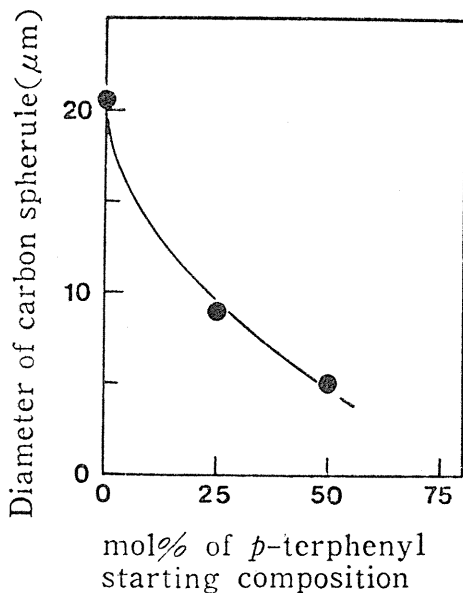


Fig. 27. Morphologies of carbons formed at  $500^{\circ}\text{C}$  by pressure pyrolysis under (a)  $300\text{kg}\cdot\text{cm}^{-2}$  and (b)  $2000\text{kg}\cdot\text{cm}^{-2}$  of anthracene.



The p-terphenyl yielded the glassy carbons with the optically isotropic and non-graphitizable character. The effect of the addition of p-terphenyl to anthracene was remarkable on the morphology and the graphitizability of the formed carbon. By the pyrolysis of anthracene at  $1000\text{kg}\cdot\text{cm}^{-2}$  and  $620^{\circ}\text{C}$ , the mesophase carbon spherulites coalesced to form carbons with mosaic texture, while by the addition of p-terphenyl to anthracene the isolated

Fig. 28. Effect of p-terphenyl addition to anthracene as starting material on diameter of formed carbon spherules.

carbon spherulites were found to be favorably formed and their diameter decreased from  $20\mu\text{m}$  to  $5\mu\text{m}$  with the increase of p-terphenyl in the mixture. Figure 28 shows the change in the diameter of carbon spherules with the addition of p-terphenyl to anthracene.

The addition of p-terphenyl to anthracene as the starting material also serves for the morphological stability of the formed carbon spherulites. Figures 29(a) and 29(b) shows the carbon spherulites synthesized at  $2000\text{kg}\cdot\text{cm}^{-2}$  and  $620^\circ\text{C}$  from anthracene and the mixture of 75mol% anthracene-25mol% p-terphenyl, respectively. By the heat treatment at  $2300^\circ\text{C}$ , these carbon spherulites change their morphologies as shown in Figure 29(c) and 29(d), respectively. The cracking along the graphitic plane (c-plane) took place especially in carbons prepared from anthracene due to the large anisotropy of the thermal expansion of graphitic layers, which leads to fragmentation of the spherulites.

Carbon spherulites obtained from mixture of anthracene with p-terphenyl held

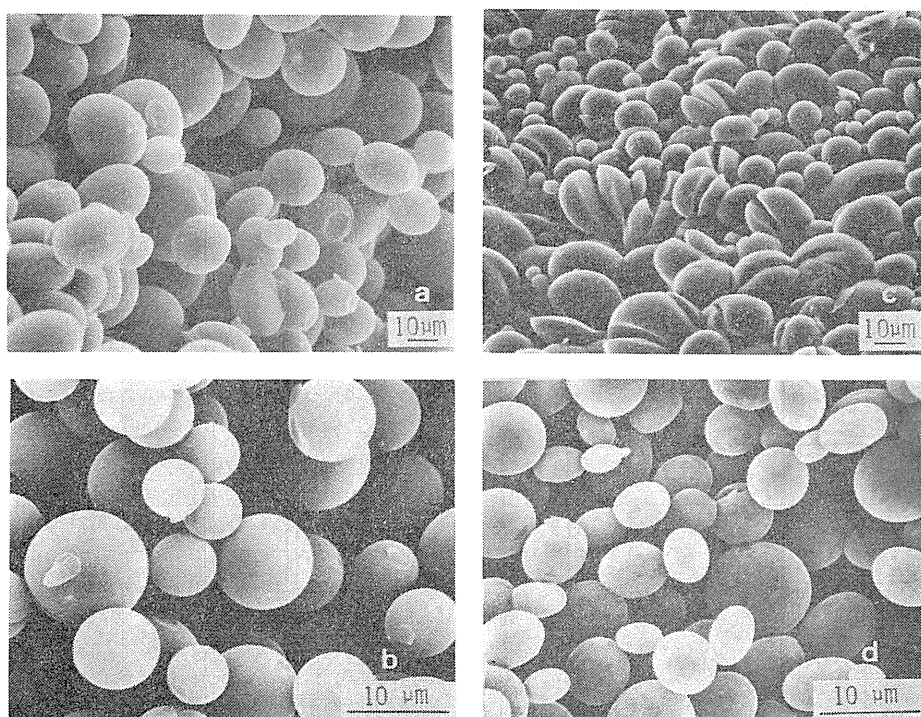


Fig. 29. Effect of p-terphenyl addition to anthracene as starting material on stability of spherical morphology of carbons by heat treatment at  $2300^\circ\text{C}$  for 1h in nitrogen flow

- (a) carbon spherules formed by pressure pyrolysis of anthracene at  $620^\circ\text{C}$  and  $2000\text{kg}\cdot\text{cm}^{-2}$ ,
- (b) carbon spherules formed by pressure pyrolysis of mixture of 75mol% anthracene-25mol% p-terphenyl at  $620^\circ\text{C}$  and  $2000\text{kg}\cdot\text{cm}^{-2}$
- (c) carbon obtained by heat treatment at  $2300^\circ\text{C}$  of carbon spherules shown in Figure 29(a)
- (d) carbon obtained by heat treatment at  $2300^\circ\text{C}$  of carbon spherules shown in Figure 29(b).

their original morphology without cracking even by the heat-treatment at 2300°C. These treated carbon spherulites are so hard that the polishing with alumina powder as abrasive is laborious. The cracking of carbon spherulites on heat-treating was restrained owing to the prevention of the development of large anisotropic graphitic layers leading to the large thermal expansion. Condensed aromatic rings offered from anthracene were bonded by the criss-cross linkage originated from p-terphenyl.

This prevention of developing graphitic layers due to the formation of cross linkages reflects the low-lying graphitizability of the formed carbon spherulites. Figure 30 demonstrates the changes of the lattice constant  $c_0$  (two times of interlayer spacing) and the crystallite size  $L_c$  of the carbon formed at 2000kg·cm<sup>-2</sup> and 620°C and subsequently heat-treated at 2300°C. It turns out from Figure 30 that the carbon spherulites with the different graphitizability can be synthesized by the adjustment of the composition of the starting organic mixture. The addition of p-terphenyl to anthracene yields the carbon spherulites with the lower degree of graphitization.

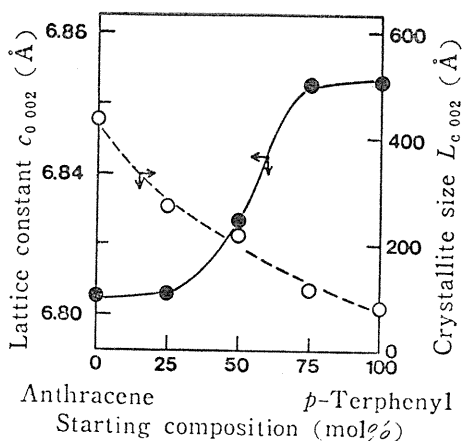


Fig. 30. Changes of lattice constant  $c_0$  and crystallite size  $L_c$  of carbons, formed from mixture with various composition of anthracene and p-terphenyl by pyrolysis at 620°C and 2000kg·cm<sup>-2</sup> for 20h and the subsequent heat treatment at 2300°C for 1h in nitrogen flow.

### 6. 3. 3. Behaviour of carbon spherulites under high pressure and temperature conditions

The spherulitic carbons formed from polydivinylbenzene and subsequently heat-treated at 2000°C were hard and less-deformable even by the heat-treatment at 40kb and 1000°C as shown in Figure 31. The spherical morphology of the carbons remained unchanged at temperatures up to 1800°C under pressures below 80kb. The carbons did not transform to diamond but was only graphitized.

On the other hand, the carbon spher-

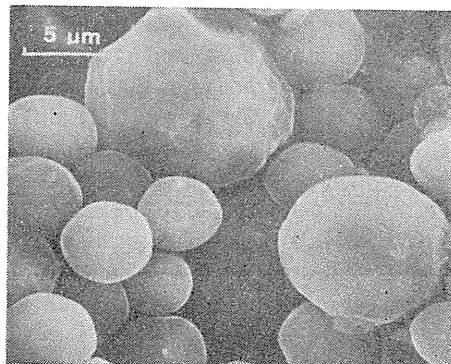


Fig. 31. Carbon spherulites, formed from divinylbenzene and heat-treated at 2000°C. and subsequently subjected to heat treatment at 40kb and 1000°C.

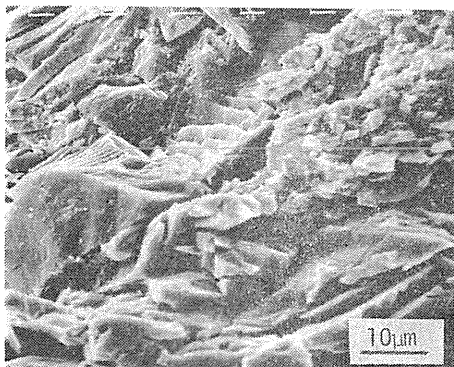


Fig. 32. Fracture surface of sintered polycrystalline diamond formed by transformation of carbon spherulites at 80kb and 2300°C.

ulites formed from the mixture of 75mol% anthracene-25mol% p-terphenyl, which have the higher degree of graphitization than that of the carbon spherulites from divinylbenzene, transformed to diamond under pressures below 80kb. Figure 32 shows the fracture surface of a sintered body of diamond formed by the transformation of the carbon spherulites at 80kb and 2300°C.

The diamond formation would be controlled at will by use of carbon spherulites with different degree of graphitization as seen in Figure 30. The detailed examination is in progress.

#### 6. 4. Conclusions

Isotropic spherulites of carbon stable above 2000°C were synthesized by the pressure pyrolysis of divinylbenzene polymer sealed in a capsule. The morphology of the synthesized carbon was pressure and temperature dependent being influenced by the state of polymerization of the starting polymer. Using a polymer prepared at atmospheric pressure and 150°C without catalyst, isolated spherulitic carbon was formed at 700°C and pressures of 1000 to 1250kg·cm<sup>-2</sup>. These spherulitic carbon were optically isotropic, hard and non-graphitizable by heat-treatment at 2000°C. Such carbons originate in the co-existence of higher and lower molecular weight products of pressure pyrolysis and the survival of cross-linkage in the original polymer. The morphology and the character of carbons formed were found to be controlled by adjusting the kind of chemical bond in the starting polymer prepared from mixture of divinylbenzene and styrene. Carbons formed by the pressure pyrolysis of copolymers rich in styrene were optically anisotropic and graphitizable after heat-treatment at 2000°C, while carbons from copolymer rich in divinylbenzene were isotropic and non-graphitizable.

The isolated anisotropic carbon spherules were synthesized by the pressure pyrolysis of anthracene at 2000kg·cm<sup>-2</sup>, while the mesophase carbons formed intermediately during the pyrolysis readily coalesced on heating under moderate pressure of 300kg·cm<sup>-2</sup> to show the complete mosaic texture. The p-terphenyl gave the glassy carbons with the optically isotropic and non-graphitizable character. By the addition of p-terphenyl to anthracene, the coalescence of the spherical carbons was restrained, and the isolated carbon spherules were produced. The size of the carbon spherules decreased from 20μm to 5μm by the addition of 50mol% p-terphenyl to anthracene as the starting material. The graphitizability of the carbon formed was found to be controlled by the selection of the mixture composition of p-terphenyl and anthracene.

It was also found that the spherical carbons with the different graphitizability could be formed efficiently with the carbon yield as high as 85% by the pressure pyrolysis. The spherulitic carbons formed from divinylbenzene or mixture of anthracene and p-terphenyl and subsequently heat-treated above 2000°C were hard

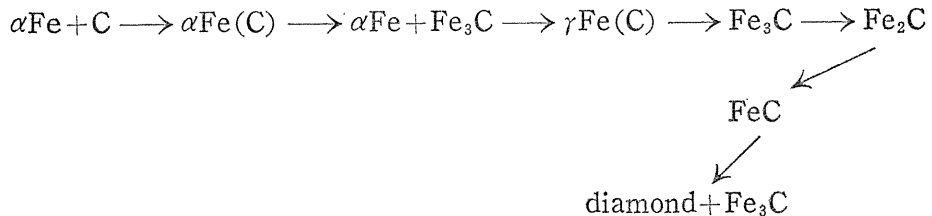
and less-deformable even by the heat-treatment under pressure. These carbons did not transform directly to diamond and were only subjected to graphitization. Diamond was synthesized through graphitization from the carbon spherulites prepared from the mixture of 75mol% anthracene and 25mol% p-terphenyl.

## 7. Behavior of iron carbides under high pressure and temperature conditions

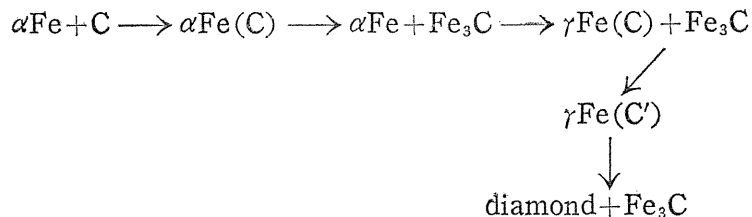
### 7. 1. Introduction

In the high pressure sample cell, the steel disks of SKH-9 are used as metal spacer, as shown in Figure 3. Iron diffusing from the metal spacers was found to react with carbon sample to form iron carbide, as mentioned in the previous chapters. Diamond formation by use of Ni or Co as solvent has been understood to proceed through their super-saturated solution (Chapter 2). On the other hand, the action of iron on carbon under high pressure and temperature conditions has not been cleared up yet in connection with the diamond formation.

The following two formation sequences of iron carbides have been proposed with increasing temperature under high pressures; by Giardini et al,<sup>5,2)</sup>



by Vereshchagin et al,<sup>5,3)</sup>



These two mechanisms are essentially similar from the viewpoint of the coexistence of Fe<sub>3</sub>C with diamond in the final stage, but differ in whether a iron carbide FeC could be formed or not in the sequence. Naka et al<sup>5,4)</sup> casted doubt on th above mechanisms with the fact that a iron carbide Fe<sub>7</sub>C<sub>3</sub> could coexist with diamond.

The diamond formation mechanism with iron has to be analysed in detail so as to elucidate the behavior of carbons under high pressure and temperature conditions. In the present chapter, the behavior and formation sequence of iron carbides under 70kb (7GPa) and 80kb were studied with regard to the diamond formation at temperatures up to 2200°C in the diamond stable region.

### 7. 2. Experimental

Figure 33 shows the arrangement of the pressure cell, which was placed in a girdle type of the high pressure apparatus in Figure 3. The well crystallized pure artificial graphite and highly pure electro-deposited iron powders were used as starting materials. A series of experiments were conducted on the desired mixtures of graphite and iron powders at temperatures up to 2200°C and pressures of 60kb (6GPa), 70kb and 80kb. The sample was heat-treated under pressure by passing the electric current directly through the sample itself in case of the direct heating (Figure 33(a)) or with a glassy carbon heater in case of the indirect heating (Figure 33(b)). The products were identified by the X-ray diffraction method, and the magnetic properties and Mössbauer effect of iron carbides formed were measured in comparison with those of the known iron carbides.

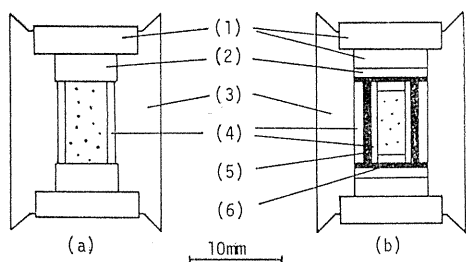


Fig. 33. Pressure cell arrangements

- (a) for direct heating,  
 (b) for indirect heating  
 (1) WC disk  
 (2) SKH-9 steel spacer  
 (3) holder (pyrophyllite)  
 (4) fired pyrophyllite sleeve  
 (5) glassy carbon heater  
 (6) graphite disk

### 7. 3. Results and Discussion

Figures 34(a) and 34(b) illustrate the changes in the relative amounts of the crystalline phases formed by the direct heating and by the indirect heating, respectively, of the mixture of 80w/o graphite and 20w/o iron (about 95 at% Carbon-5 at% iron) for 10 min under 80kb (8GPa).  $\alpha$ -iron reacted almost completely with graphite to form cementite ( $\text{Fe}_3\text{C}$ ) up to around 1000°C. With increase in the heat treatment temperature, the formation of the carbide  $\text{Fe}_7\text{C}_3$  took place by the reaction of  $\text{Fe}_3\text{C}$  with residual graphite. The relative amount of  $\text{Fe}_7\text{C}_3$  decreased at 1500°C, which was followed by the formation of diamond in case of the direct heating (Figure 34(a)). The carbide  $\text{Fe}_7\text{C}_3$  thus formed below 1500°C has the same crystallographic structure as  $\text{Cr}_7\text{C}_3$  or  $\text{Mn}_7\text{C}_3$ <sup>55)</sup> and found to have the stoichiometry by the chemical analysis. The Curie temperature of the carbide  $\text{Fe}_7\text{C}_3$  was to be 250°C. Above 1600°C, the carbide  $\text{Fe}_7\text{C}_3$  was found to be stabilized by the formation of solid solution with Cr (ca. 4wt%), Mo (ca. 5wt%), W (ca. 6wt%) and

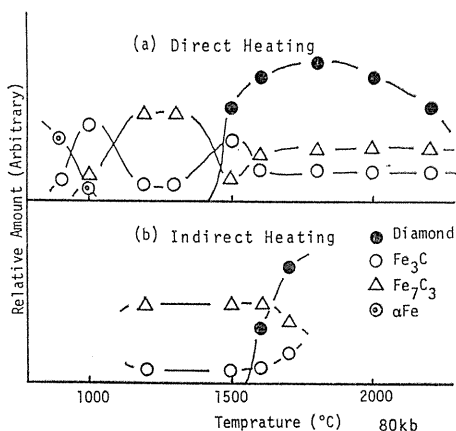


Fig. 34. Changes in relative amounts of phases with heat treatment at 80kb

- (a) by direct heating and  
 (b) by indirect heating.

V (ca. 2wt%) of minor constituents diffusing out from the steel SKH-9 spacer in the pressure cell as shown in Figure 33(a). A sequential formation of iron carbides and diamond became more understandable in case of indirect heating as in Figure 34(b).

Figure 35 shows the magnetization curves of the specimens directly heat-treated under 80kb. The magnetization curves indicate the presence of  $\text{Fe}_3\text{C}$  ( $T_c$ ; 210°C) with  $\alpha$ -iron at 1000°C and the substantial formation of  $\text{Fe}_7\text{C}_3$  ( $T_c$ ; 250°C) at 1300°C and then the coexistence of the carbide of  $\text{Fe}_7\text{C}_3$  solid solution with  $\text{Fe}_3\text{C}$  reformed at 1800°C. The magnetic properties of the carbide were measured by the Farady method in an applied field of 0.5T in the temperature range from 77K to 600K. The carbide of  $\text{Fe}_7\text{C}_3$  solid solution is ferromagnet with Curie temperature of 120°C and found to have the magnetic moment of  $1.7\mu_B$  per iron atom from the comparison of the saturation magnetization of the carbide and  $\alpha$ -iron which were formed by the decomposition of the carbide at 800°C. The magnetic separation of the  $\text{Fe}_7\text{C}_3$  solid solution could be performed easily from the residual graphite powder, but not from diamond.

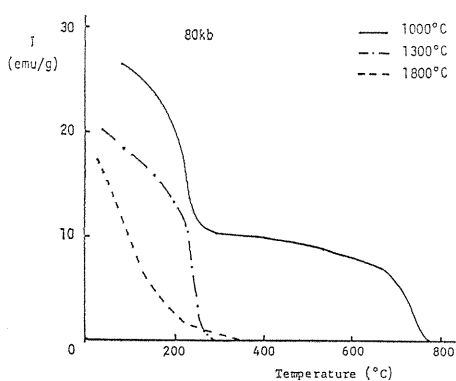


Fig. 35. Magnetization curves of products formed at 80kb by direct heating of mixture of 80 w/o graphite-20 w/o iron.

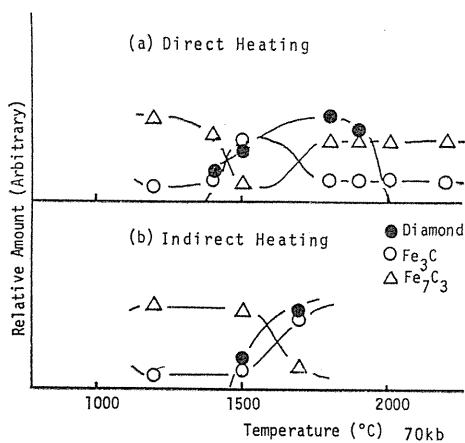


Fig. 36. Changes in relative amounts of phases with heat treatment at 70 kb  
(a) by direct heating and  
(b) by indirect heating.

Figure 36 shows changes of the relative amounts of the crystalline phases in specimen treated under 70kb by the direct heating (Figure 36(a)) or the indirect heating (Figure 36(b)) of the mixture 80w/o graphite-20w/o iron for 10min. The behaviors of iron carbides under 70kb were found to be similar to those under 80kb, except that the onset temperature of the reformation of  $\text{Fe}_3\text{C}$  became slightly lower under 70kb, that is, the decomposition of  $\text{Fe}_7\text{C}_3$  took place at lower temperature than under 80kb.

The Mössbauer spectra of pure  $\text{Fe}_7\text{C}_3$  and the  $\text{Fe}_7\text{C}_3$  solid solution are shown in Figure 37. Iron metal was used for the velocity calibration and as the standard for the datum of the chemical shift. It turns out that there are three ion sites in

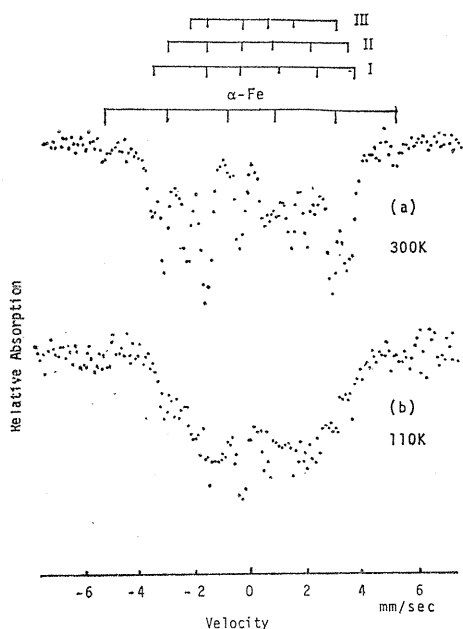


Fig. 37. Mössbauer spectra of stoichiometric  $\text{Fe}_7\text{C}_3$  and  $\text{Fe}_7\text{C}_3$  solid solution

pure  $\text{Fe}_7\text{C}_3$ , of which population ratio is about 1:2:2. The data are considered to be in good agreement with those reported by Herbstein and Snyman,<sup>55)</sup> except for a little difference in the population ratio. On the other hand, the carbide of  $\text{Fe}_7\text{C}_3$  solid solution showed a confused magnetic hyperfine structure (Figure 36 (b)). It was impossible to divide the spectrum into each components, but apparently there exists equal number to or larger number of iron sites than that in pure, stoichiometric  $\text{Fe}_7\text{C}_3$  itself. The carbide  $\text{Me}_7\text{C}_3$  (Me; 85w/oFe, 5w/oCr, 5w/oMo and 5w/oW) synthesized at 1700°C under 70kb had the Curie temperature of 125°C and the X-ray diffraction pattern which are close to those of the carbide of the  $\text{Fe}_7\text{C}_3$  solid solution associated with diamond above 1600°C under 70kb and 80kb in this work. This result might suppose that both of the carbides had almost the same chemical composition and the isost-structure.

Under 80kb, the mixture of the synthesized  $\text{Fe}_7\text{C}_3$  and graphite (about 5 at% Fe-95 at% C) decomposed only in part to form a little of cementite ( $\text{Fe}_3\text{C}$ ) and diamond after the heat treatment at 1700°C for 30min, while under 70kb the same mixture sample finally changed at 1500°C for 30min to cementite and trace of diamond, and to cementite and graphite (not diamond) even at 1450°C under the pressure of 60kb. It follows from the fact that the carbide  $\text{Fe}_7\text{C}_3$  becomes less stable with lowering the pressure and more stable by the formation of solid solution with metals such as Cr, Mo and W as shown in Figure 34 and 36.

It may be proposed that  $\text{Fe}_7\text{C}_3$  decomposes to leave  $\text{Fe}_3\text{C}$  and diamond under pressures above 70kb. Eventually, in this study, formed diamond coexisted with the carbide  $\text{Fe}_7\text{C}_3$  solid solution but not with  $\text{Fe}_3\text{C}$ , as mentioned in the previous chapters.

The existence of  $\text{Fe}_7\text{C}_3$  with diamond casts doubt on the mechanism of the diamond formation in the Fe-C system at high temperatures and pressures by the scheme proposed so far.<sup>56)</sup> The more detailed study on the stability of  $\text{Fe}_7\text{C}_3$  under pressures should be required in relation to the phase diagram by Zhukov et al<sup>55)</sup> who described the instability of  $\text{Fe}_3\text{C}$  in  $\text{Fe}_7\text{C}_3$ -C system under 80kb.

#### 7. 4. Conclusions

The present chapter dealt with the behavior of iron carbides, at pressures up to 80kb and temperatures up to 2200°C in the diamond stable region, which has attention as to the mechanism of the diamond formation in the carbon-iron system. At 80kb,  $\alpha$ -iron reacts below 1000°C with graphite to form  $\text{Fe}_3\text{C}$ , which subsequently reacts with residual graphite to give  $\text{Fe}_7\text{C}_3$  at around 1200°C. The stoichiometric

$\text{Fe}_7\text{C}_3$  with Curie temperature of  $250^\circ\text{C}$  thus formed decomposes in part to leave  $\text{Fe}_3\text{C}$  and diamond above  $1500^\circ\text{C}$ . The carbide  $\text{Fe}_7\text{C}_3$  becomes less stable with lowering the pressure and is stabilized by the formation of solid solution with metals such as Cr, Mo and W. The experimental evidence of the coexistence of  $\text{Fe}_7\text{C}_3$  (not  $\text{Fe}_3\text{C}$ ) with diamond as mentioned in the previous chapters casts doubt on the mechanism of the diamond formation so far reported.

## 8. Summary

The behaviors of the carbeneous materials under high pressure and temperature conditions have not yet been understood in spite of the importance for the selection of the most suitable starting carbon material in order to synthesize diamond efficiently. In this paper, it has been pointed out that the electro-thermal analysis under pressure can be applied to the in situ observations of the behavior of the carbon materials and the diamond formation by controlling the dimension and the charge density of the starting carbon sample.

It was found that the diamond formation depended strongly on the nature of carbeneous materials, especially on the degree of graphitization. The onset temperature of the diamond formation could be lowered to some extent by using the carbon material with high crystallinity, but raised by the introduction of the distortion onto graphite crystals.

The pressure of 120kb (12GPa) was essential to convert graphite to diamond instantaneously without any induction period. Under the pressure below 120kb, the induction period prior to the conversion to diamond and the apparent crystallization time increased with the decrease of the applied pressure. These results confirm the usefulness of the electro-thermal analysis for the efficient diamond production under a controlled condition.

The amorphous glassy carbon with the characteristic bond nature was found to transform into diamond only through the formation of the metastable graphite in accordance with the Ostwald's step rule. This phenomenon could be observed also on the synthesized carbon spherulites with lower degree of graphitization. The carbon spherulites synthesized in this work can be applicable to the controlled diamond production, since the bond nature of the formed carbon materials is adjustable by the selection on the original organic compound.

Although behavior of the carbon materials could be elucidate in this work by the electro-thermal analysis under pressure, the more detailed study on various kinds of carbon-metal systems under pressure should be required in regard to the diamond formation.

## Acknowledgement

This work was supported in part by the Grant-in-Aid for Scientific Research from the Ministry of Education, Science and Culture.

## References

- 1) H. Moissan: *Compt. Rend.*, 118 (1894) 320.
- 2) F. P. Bundy, H. T. Hall, H. M. Strong and R. H. Wentorf, Jr.: *Nature*, 176 (1955) 51.
- 3) F. P. Bundy: *Science*, 137 (1962) 1057.
- 4) F. P. Bundy, H. P. Bovenkerk, H. M. Strong and R. H. Wentorf, Jr.: *J. Chem. Phys.*, 35 (1961) 383.
- 5) R. Berman and F. Simon: *Z. Electrochem*, 59 (1955) 333.
- 6) C. S. Kennedy and G. C. Kennedy: *J. Geophys. Res.*, 81 (1976) 2667.
- 7) P. S. DeCarli and J. C. Jamieson: *Science*, 133 (1961) 182.
- 8) F. P. Bundy: *J. Chem. Phys.*, 618 (1963) 631.
- 9) F. P. Bundy and J. S. Kasper: *J. Chem. Phys.*, 46 (1967) 3437.
- 10) H. P. Bovenkerk, F. P. Bundy, H. T. Hall, H. M. Strong and R. H. Wentorf, Jr.: *Nature*, 184 (1959) 1094.
- 11) H. M. Strong and R. E. Hanneman: *J. Chem. Phys.*, 75 (1971) 1838.
- 12) H. M. Strong and R. H. Wentorf, Jr.: *Naturwissenschaften*, 59 (1972) 1.
- 13) W. G. Eversole: *Canadian Pat.* 628567 (1961).
- 14) H. J. Hibshman: *U. S. Pat.* 3371996 (1968).
- 15) J. C. Angus, H. A. Will and W. S. Stanko: *J. Appl. Phys.*, 39 (1968) 2915.
- 16) B. V. Deryagin, V. G. Lyuttsan, D. V. Fedoseev and V. A. Ryabov: *Dokl. Akad. Nauk. SSSR*, 190 (1970) 86.
- 17) S. Aisenberg and R. Chabot: *J. Appl. Phys.*, 42 (1971) 2953.
- 18) B. V. Spitsyn, L. L. Bouilov and B. V. Derjaguin: *J. Cryst. Growth*, 52 (1981) 219.
- 19) C. R. Houska and B. E. Warren: *J. Appl. Phys.*, 25 (1954) 1503.
- 20) H. G. Drickamar: *J. Sci. Instrum.*, 41 (1970) 1667.
- 21) H. T. Hall: *Nat. Bur. Stand. (U. S.) Spec. Pub.*, 326 (1971) 313.
- 22) H. M. Strong and F. P. Bundy: *Rev.*, 115 (1959) 278.
- 23) L. H. Cohen, W. Klement, Jr. and G. C. Kennedy: *Phys. Rev.*, 145 (1966) 519.
- 24) S. Naka, K. Horii, Y. Takeda and T. Hanawa: *Nature*, 259 (1976) 38.
- 25) R. H. Wentorf, Jr.: *J. Phys. Chem.*, 69 (1965) 3063.
- 26) F. P. Bundy and J. S. Kasper: *J. Chem. Phys.*, 46 (1967) 3437.
- 27) S. Naka, Y. Suwa, Y. Takeda and S. Hirano: *J. Chem. Soc., Jpn (Chem. and Ind. Chem.)*, 1981 (1981) 1468.
- 28) S. Naka, S. Hirano, K. Shimono and Y. Takeda: *J. Jpn Soc. Powder and Powder Metallurgy*, 25 (1978) 268.
- 29) S. Hirano: *Thesis for Dr. Eng.* (1970).
- 30) T. Noda, M. Inagaki, S. Hirano and K. Amanuma: *Bull. Chem. Soc. Japan*, 41 (1968) 1245.
- 31) S. Hirano, K. Shimono and S. Naka: *J. Mat. Sci.*, (to be published) (1982).
- 32) S. Tolansky and W. L. Wilcock: *Proc. Roy. Soc.*, A191 (1947) 182.
- 33) A. Halperin: *Proc. Phys. Soc.*, 67 (1954) 538.
- 34) S. Tolansky and I. Sunagawa: *Nature*, 185 (1960) 203.
- 35) C. K. R. Varma: *Phil. Mag.*, 16 (1967) 611, 621, 959.
- 36) M. Omar and M. Kenawi: *Phil. Mag.*, 2 (1957) 859.
- 37) F. C. Frank, K. E. Pettick and E. M. Wilks: *Phil. Mag.*, 3 (1958) 1262.
- 38) F. C. Frank and K. E. Pettick: *Phil. Mag.*, 3 (1958) 1273.
- 39) E. M. Wilks: *Phil. Mag.*, 6 (1961) 1089.
- 40) A. R. Patel and S. Ramanathan: *Phil. Mag.*, 2 (1962) 1305.
- 41) A. R. Patel, K. N. Goswami and C. C. Desai: *Phil. Mag.*, 10 (1964) 931.
- 42) A. R. Lang: *Proc. Roy. Soc.*, A378 (1964) 234.
- 43) J. J. Kipling, J. N. Sherwood, P. V. Shooter and N. R. Thompson: *Carbon*, 1 (1964) 315.
- 44) P. L. Walker, Jr. and A. Weinstein: *Carbon*, 5 (1967) 13.
- 45) A. S. Kotosonov, V. A. Vinnikov, V. I. Frolor and B. G. Ostronov: *Dokl. Akad. Nauk*,

- SSSR, 185 (1969) 1316.
- 46) H. Marsh, F. Datchille, J. Melvin and P. L. Walker, Jr.: Carbon, 9 (1971) 159.
  - 47) P. W. Whang, F. Datchille and P. L. Walker, Jr.: High Temp. High Press., 6 (1974) 123.
  - 48) S. Hirano, F. Datchille and P. L. Walker, Jr.: High Temp. High Press., 5 (1973) 207.
  - 49) S. Hirano, M. Ozawa and S. Naka: J. Mat. Sci., 16 (1981) 1989.
  - 50) S. Hirano, M. Ozawa and S. Naka: Proc. 8th Int'l Conf. High Pressure (in press).
  - 51) S. Hirano, I. Ohta and S. Naka: J. Chem. Soc. Jpn, 1981 (1981) 1356.
  - 52) A. A. Giardini and J. E. Tydings: Am. Mineral., 47 (1962) 1393.
  - 53) A. L. F. Vereschagin, L. E. Shtereberg and V. N. Slesarev: Soviet Phys. Dokl., 15 (1970) 556.
  - 54) S. Naka, A. Tsuzuki, Y. Takeda and S. Hirano: Ferrites; Proc. 3rd Int'l Conf. on Ferrites 929 (1981).
  - 55) F. H. Herbststein and J. A. Snyman: Inorg. Chem., 3 (1964) 894.
  - 56) A. A. Zhukov, L. E. Shterenberg, V. A. Shalachov, V. K. Thomas and N. A. Beregovskaya: Acta Metal., 21 (1973) 195.